V4 Japan project

Report 08-08-2016 DRAFT 2

1. Samples

1.1 Labeling and basic physical properties

Samples from AGH taken on Jan-12. 2016

Two types of samples- **tubes and tension bars** after tension test (halves).

Tension bars- halves				**Bulk density** g/cm3
Ax30		extruded	1	
		and lathed	2	1824
			3	
			4	
			5	
ZEK100		extruded	1	
		and lathed	2	1805
			3	
			4	
			5	
MgCa0.8		extruded	1	
		and lathed	2	
			3	
			4	
			5	1793

		Preparation technology	**Spec. No.**	**Outer diameter (mm)**		**Inner diameter (mm)**		**Wall (mm)**		**Bulk density**
										g/cm3
Tubes				mean	s.d.	mean	s.d.	mean	s.d.	
Ax30		extrusion	-	5.29	0.06	4.24	0.08	0.51	0.09	1711
ZEK100		extrusion	-	4.84	0.30	3.86	0.23	0.56	0.17	1699
Al36		extrusion	-	5.01	0.11	4.09	0.11	0.41	0.06	1457
AZ31		extrusion	-	4.97	0.02	4.04	0.01	0.53	0.06	1547
MgCa0.8		extrusion	-	4.99	0.01	3.89	0.01	0.51	0.01	1599

Preparation

Before further analyses samples were grinded and polished.

2. Optical analysis of tension bars

All samples are characterized by a distributed porosity and defects. They are recognized as black dots in optical images. Defects tend to be accumulated in neck zones whereas are less present closer to the test piece head. Also, striation occurs in the direction of the tension loading. In the following, typical optical images are provided for distinct places in the sample and image analysis results are summarized in Tabs. 1-4 in Section 2.5.

2.1. Ax30 Tension bars

Ax30.2 **Neck zone** **Test piece head**

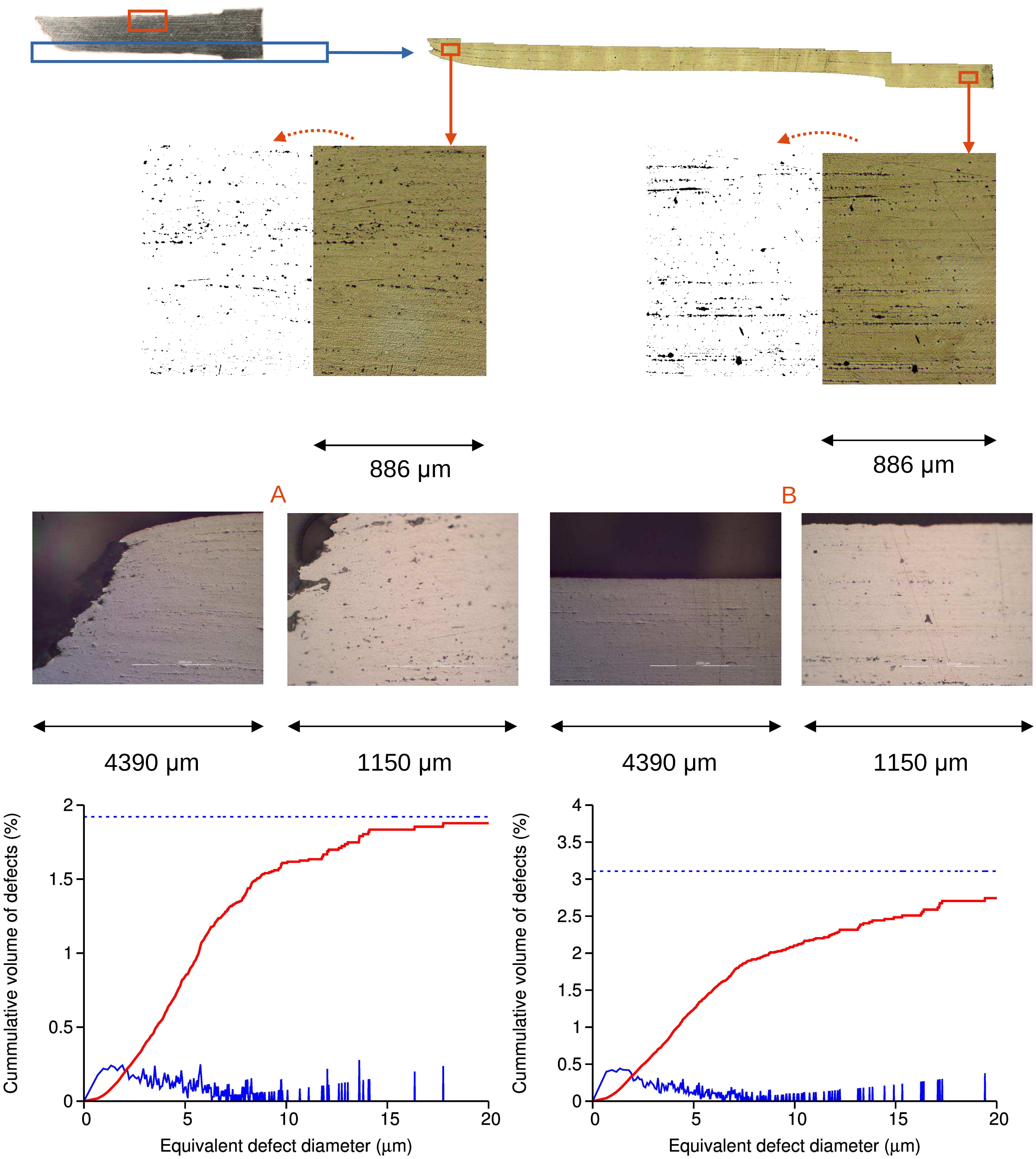

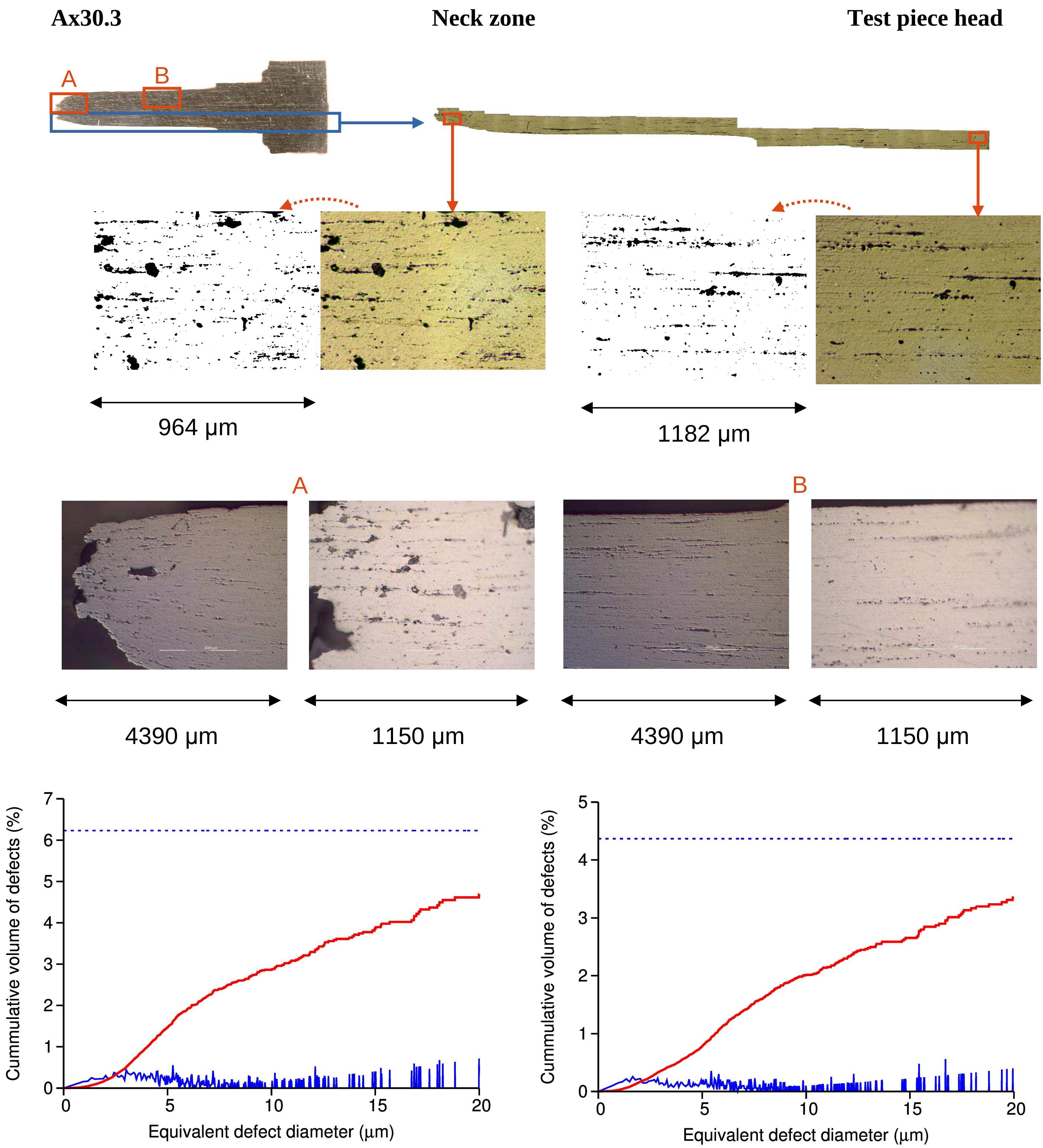
Ax30.3
Neck zone
Test piece head
A
B
964 µm
1182 µm
A
B
4390 µm
1150 µm
4390 µm
1150 µm
Cummulative volume of defects (%)
Equivalent defect diameter (µm)
Cummulative volume of defects (%)
Equivalent defect diameter (µm)

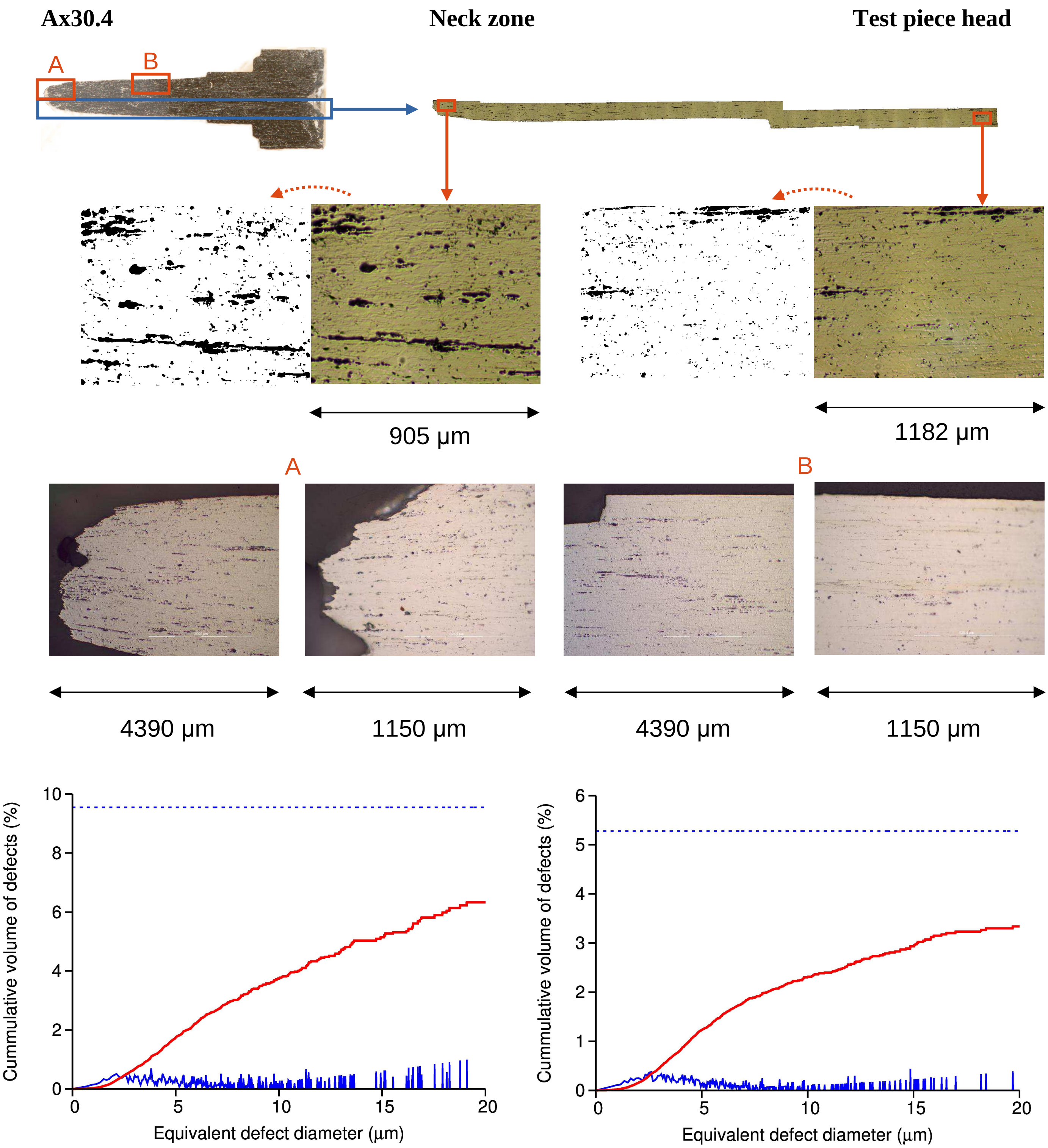
Ax30.4
Neck zone
Test piece head
A
B
905 µm
1182 µm
A
B
4390 µm
1150 µm
4390 µm
1150 µm
Cummulative volume of defects (%)
Equivalent defect diameter (µm)
Cummulative volume of defects (%)
Equivalent defect diameter (µm)

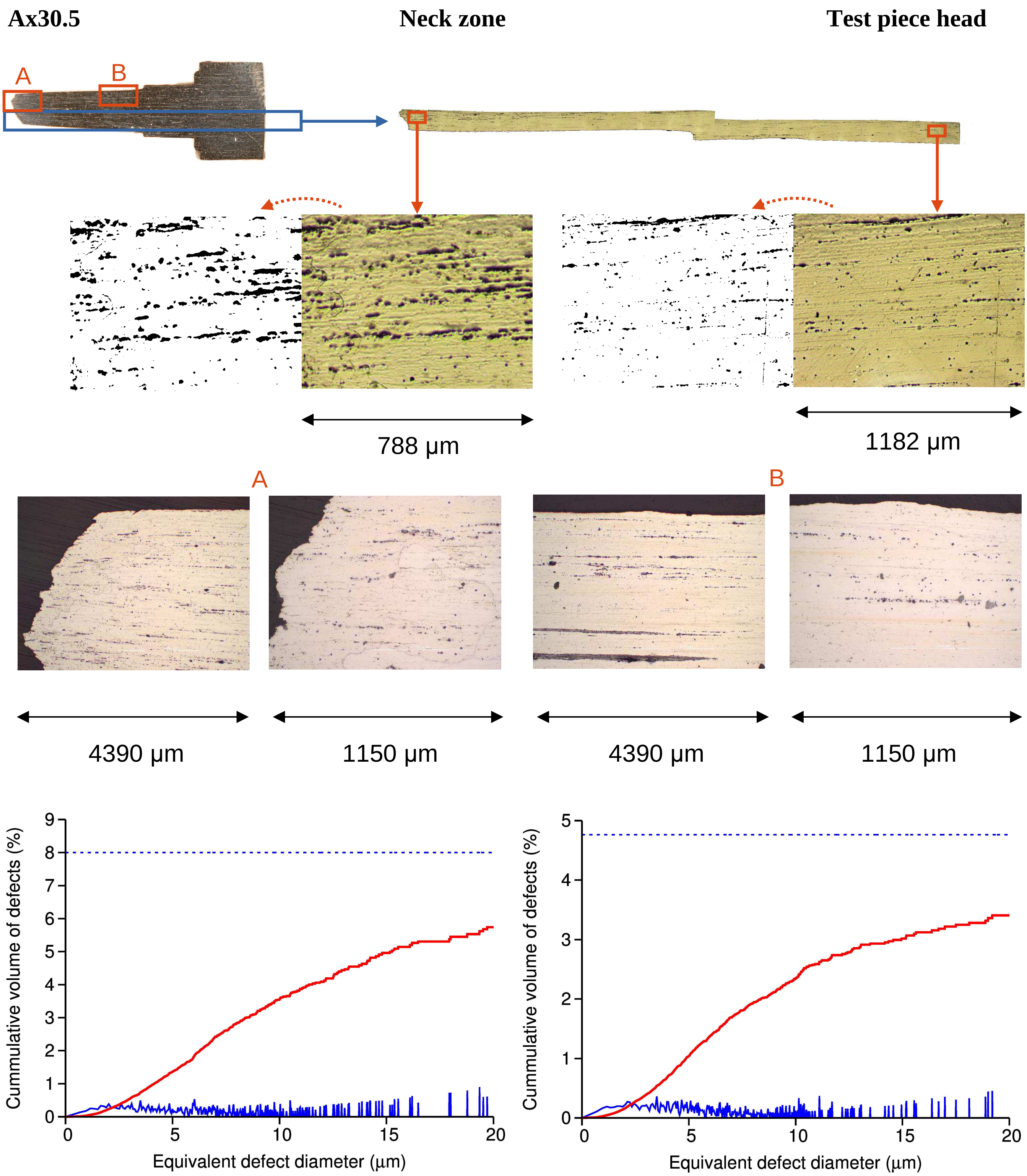

Ax30.5
Neck zone
Test piece head
A
B
788 µm
1182 µm
A
B
4390 µm
1150 µm
4390 µm
1150 µm
Cummulative volume of defects (%)
Equivalent defect diameter (µm)
0 5 10 15 20
0 1 2 3 4 5 6 7 8 9
Cummulative volume of defects (%)
Equivalent defect diameter (µm)
0 5 10 15 20
0 1 2 3 4 5

2.2. MgCa08 Tension bars

MgCa08.2 **Neck zone** **Test piece head**

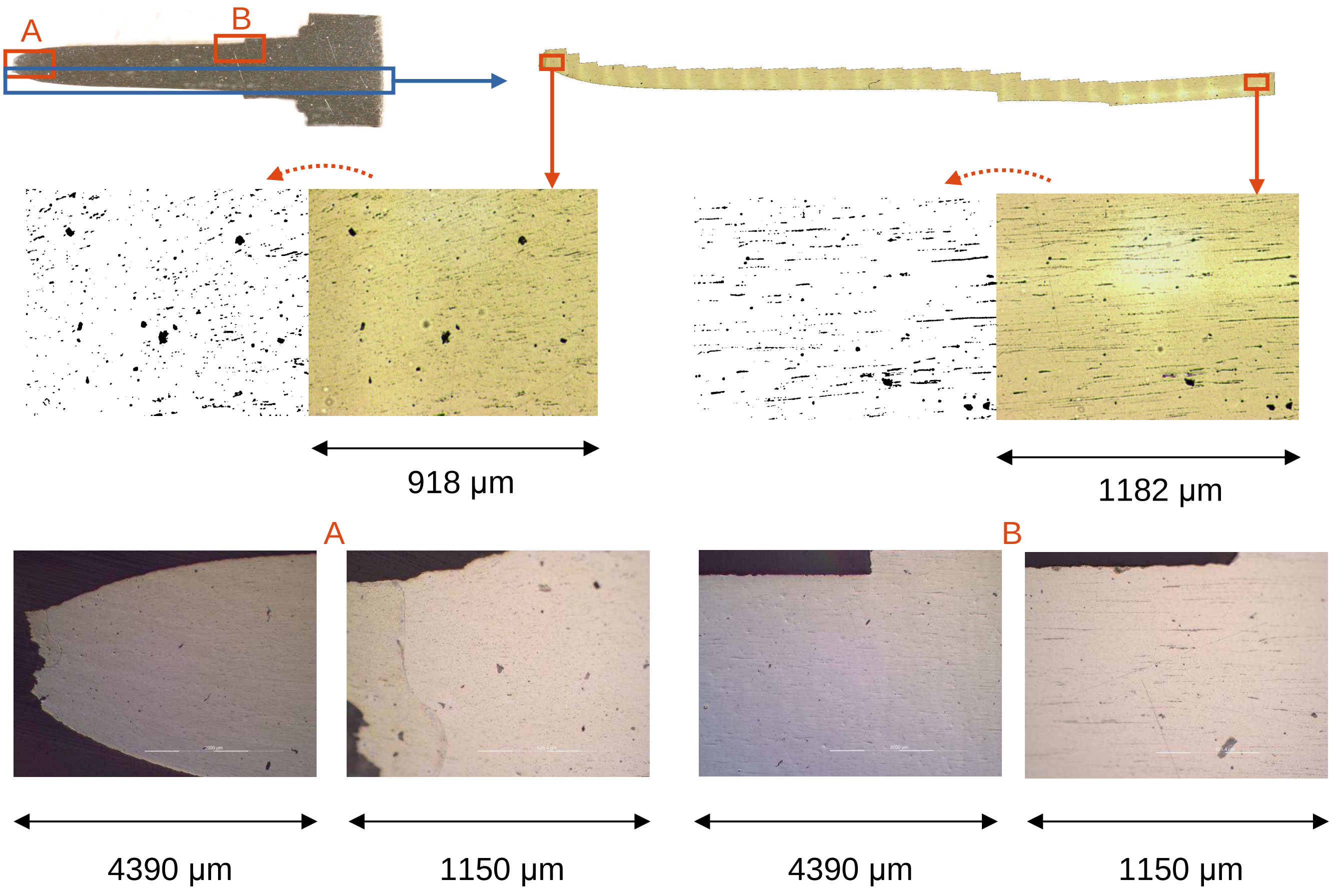

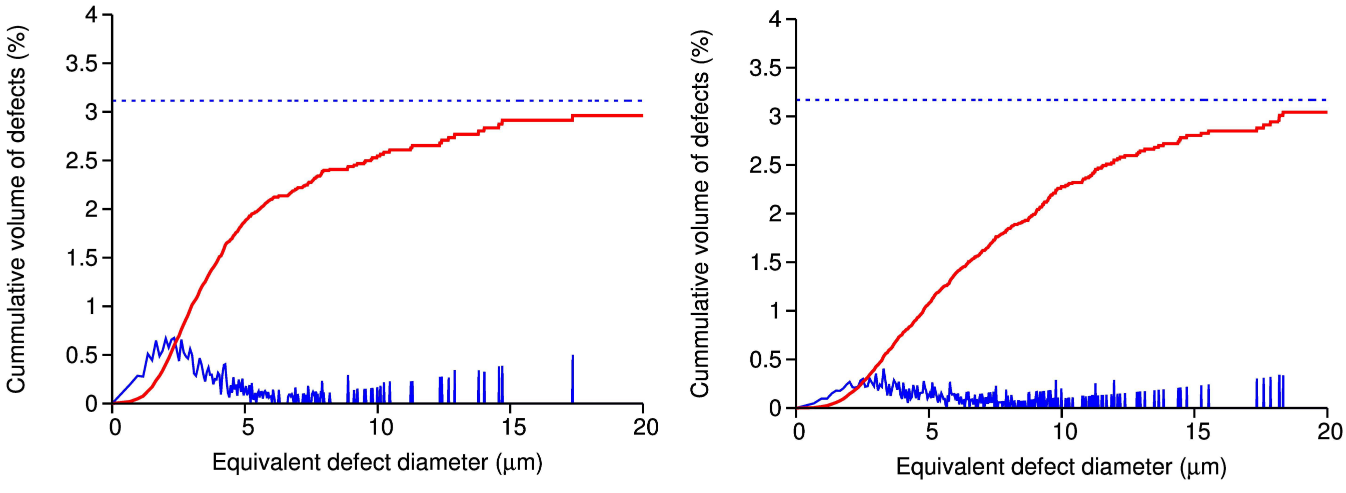

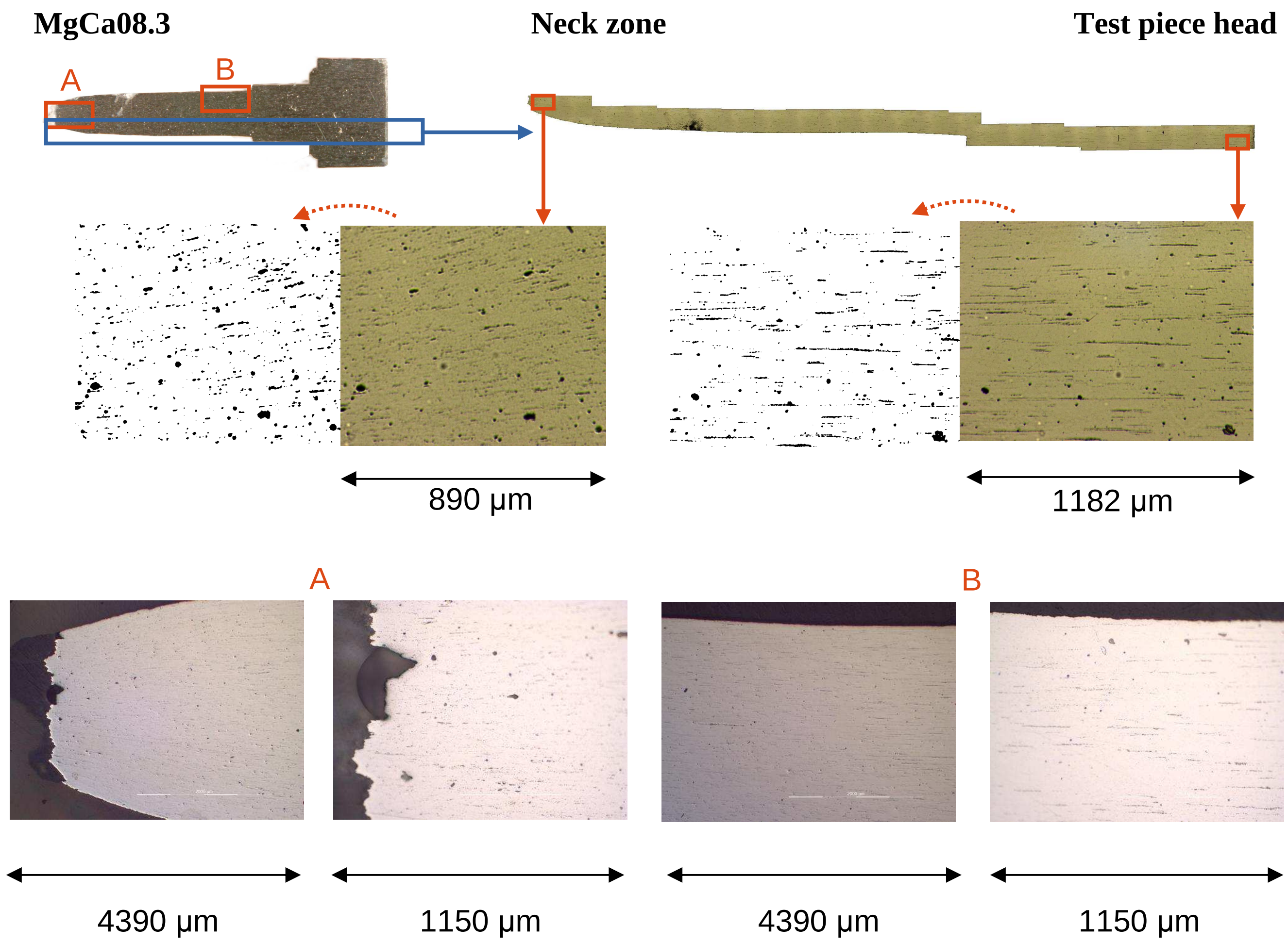
MgCa08.3
Neck zone
Test piece head
A
B
890 µm
1182 µm
A
B
4390 µm
1150 µm
4390 µm
1150 µm

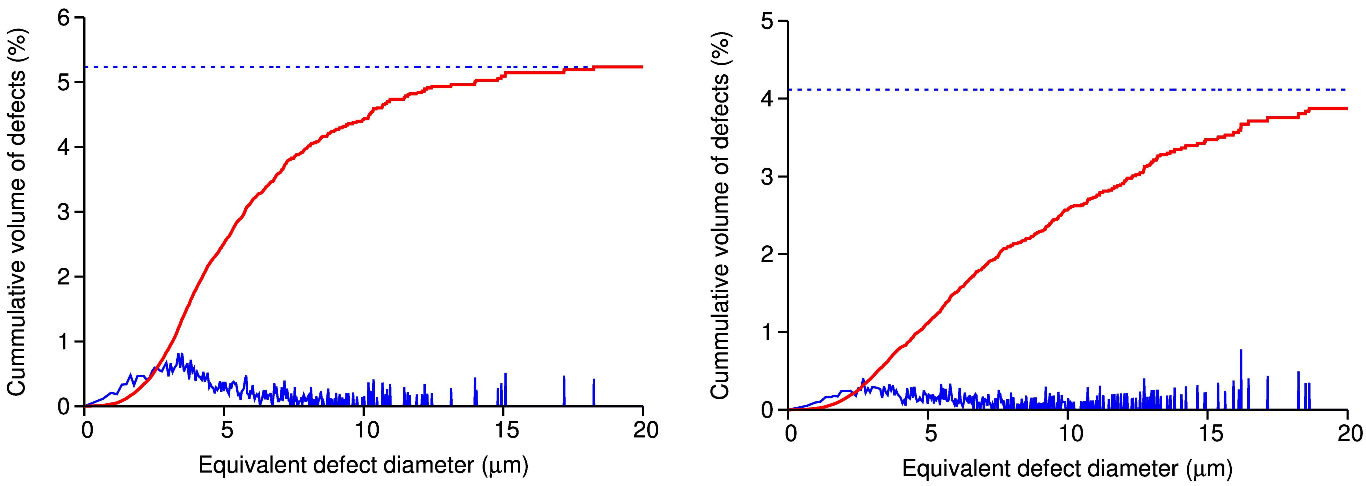
Cummulative volume of defects (%)
Equivalent defect diameter (µm)
0
1
2
3
4
5
6
5
10
15
20
Cummulative volume of defects (%)
Equivalent defect diameter (µm)

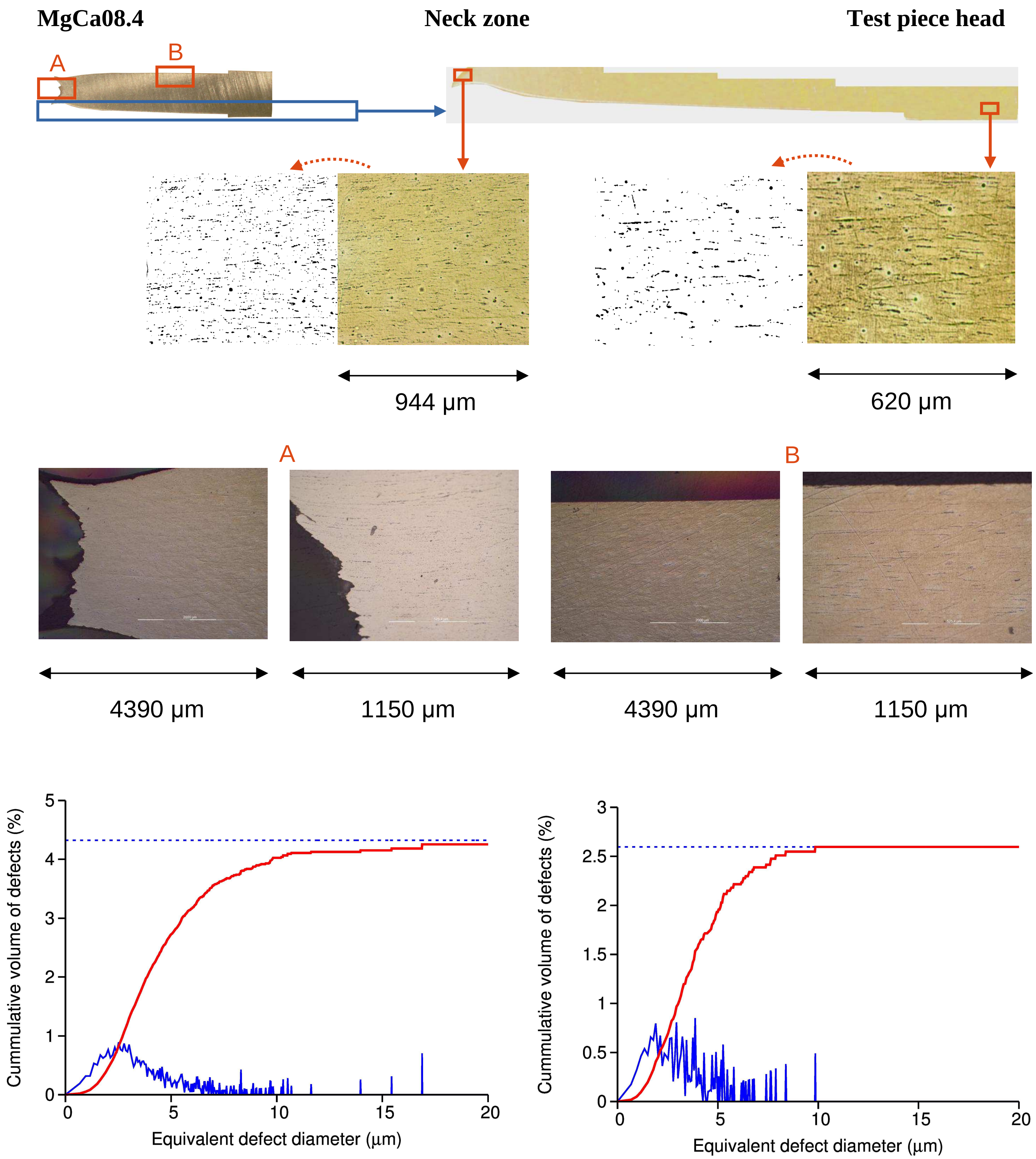
MgCa08.4
Neck zone
Test piece head
A
B
944 µm
620 µm
A
B
4390 µm
1150 µm
4390 µm
1150 µm
Cummulative volume of defects (%)
Equivalent defect diameter (µm)
Cummulative volume of defects (%)
Equivalent defect diameter (µm)

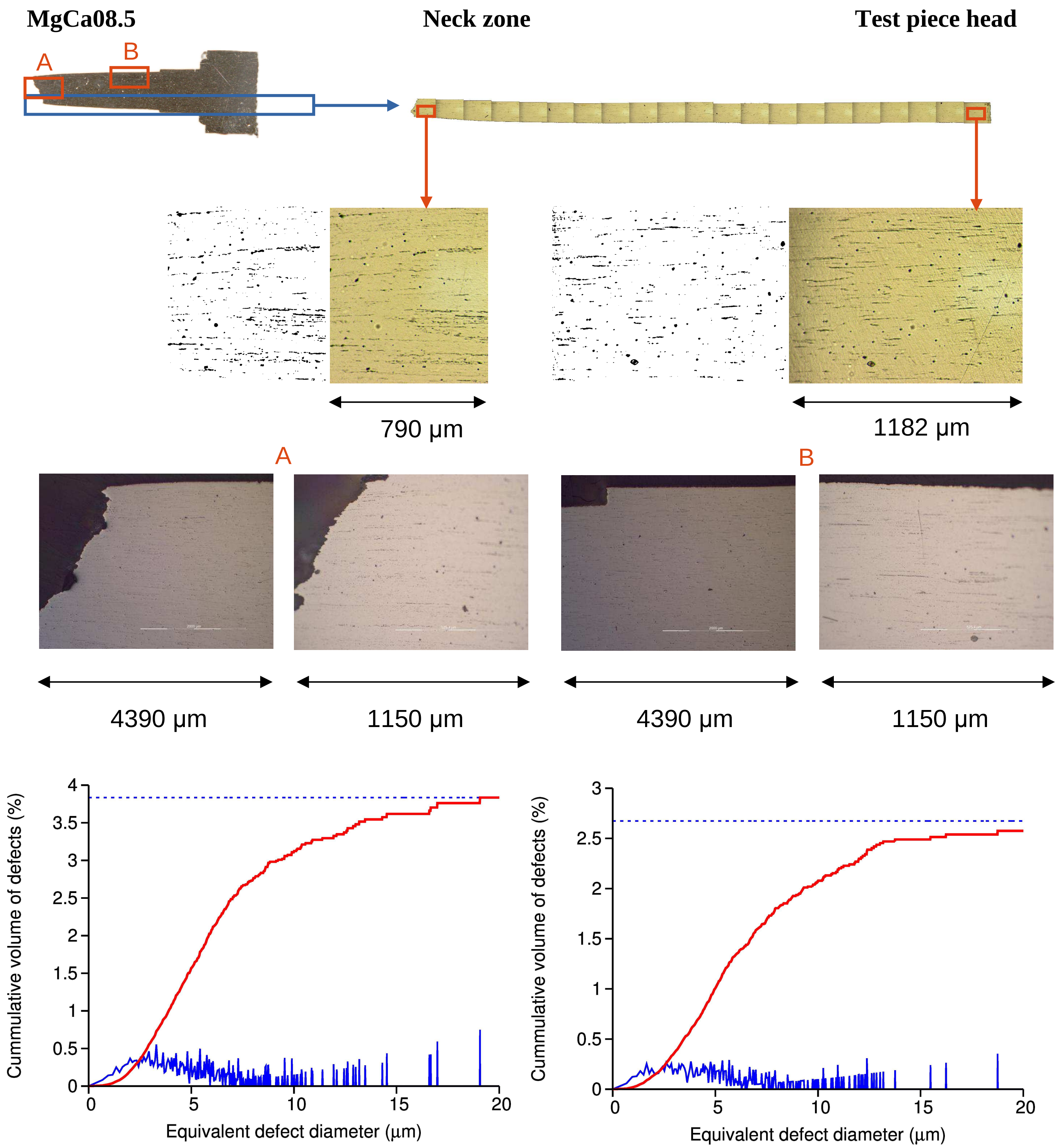
MgCa08.5
Neck zone
Test piece head
A
B
790 µm
1182 µm
A
B
4390 µm
1150 µm
4390 µm
1150 µm
Cummulative volume of defects (%)
Equivalent defect diameter (µm)
Cummulative volume of defects (%)
Equivalent defect diameter (µm)

2.3. ZEK100 Tension bars

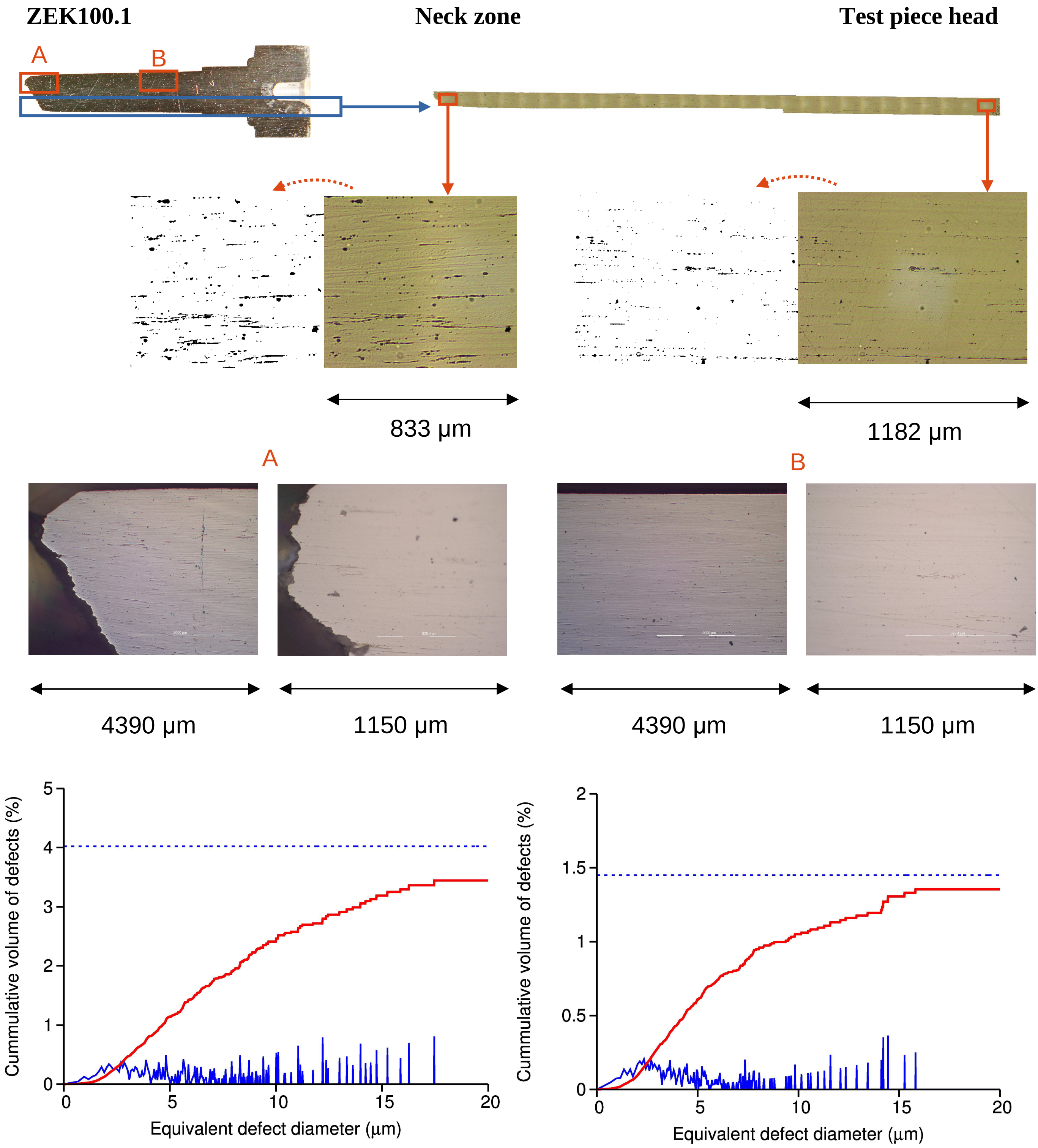

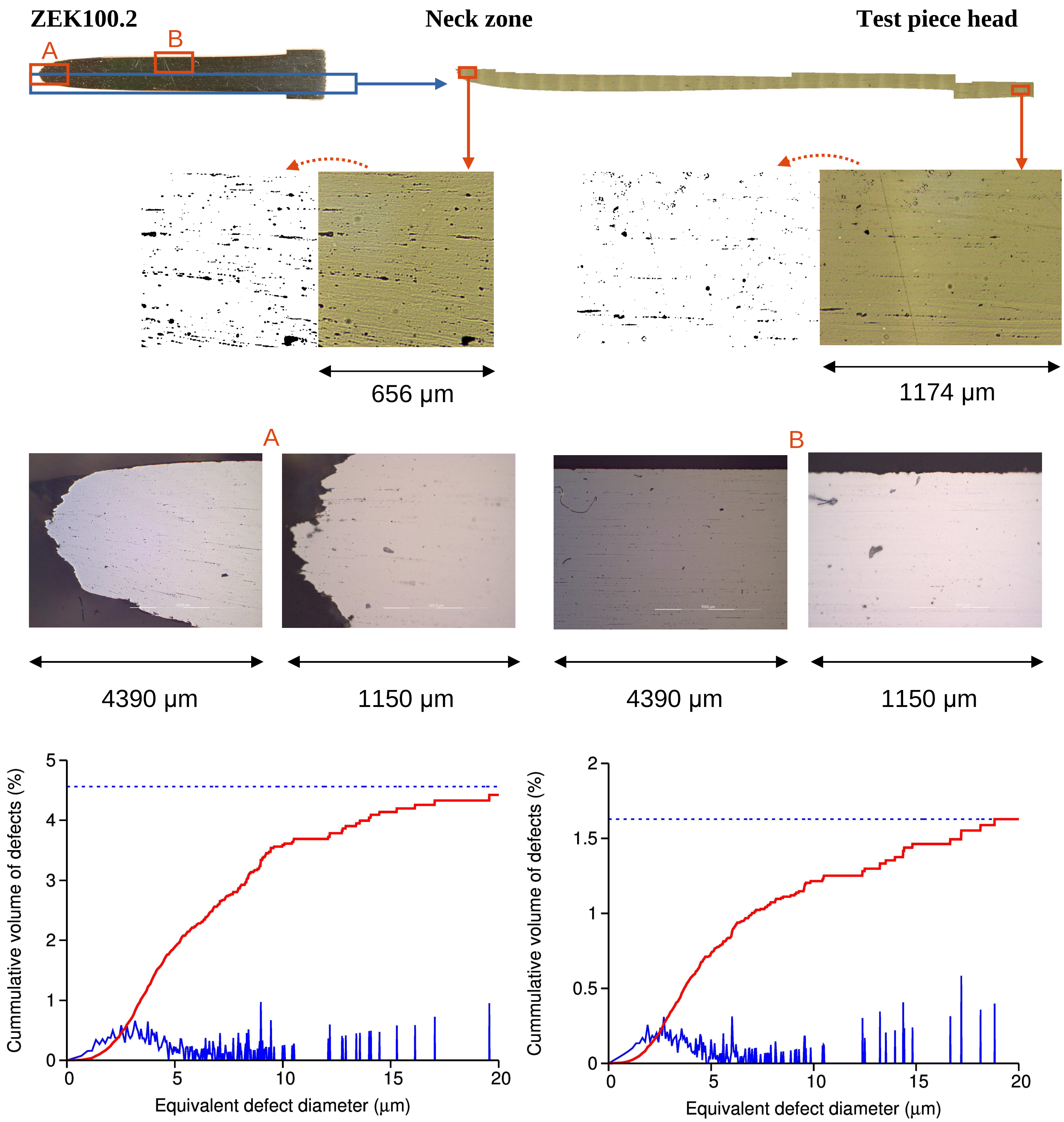
ZEK100.2
Neck zone
Test piece head
A
B
656 μm
1174 μm
4390 μm
1150 μm
4390 μm
1150 μm
Cummulative volume of defects (%)
Equivalent defect diameter (μm)
Cummulative volume of defects (%)
Equivalent defect diameter (μm)

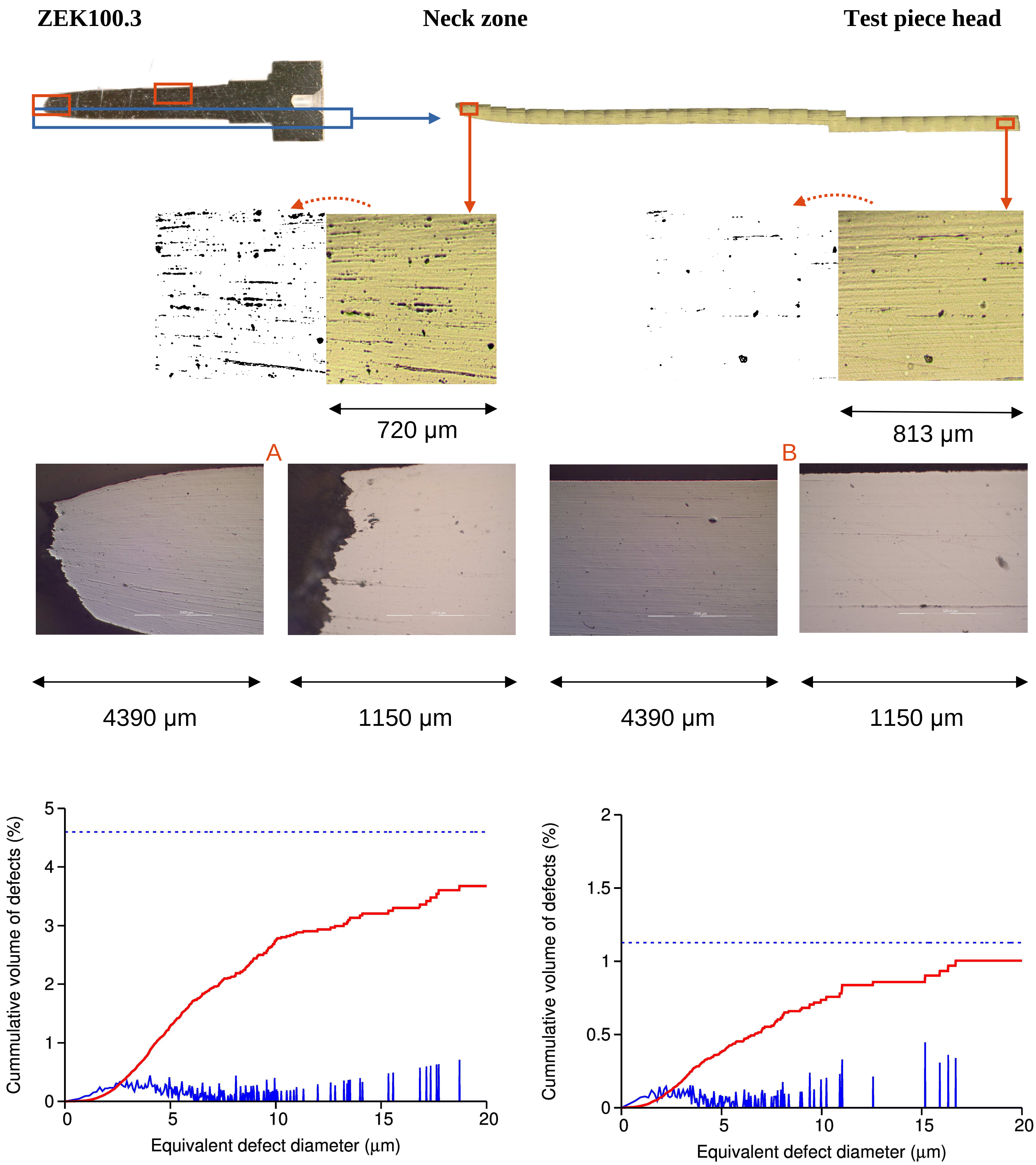
ZEK100.3
Neck zone
Test piece head
720 µm
813 µm
A
B
4390 µm
1150 µm
4390 µm
1150 µm
Cummulative volume of defects (%)
Equivalent defect diameter (µm)
Cummulative volume of defects (%)
Equivalent defect diameter (µm)

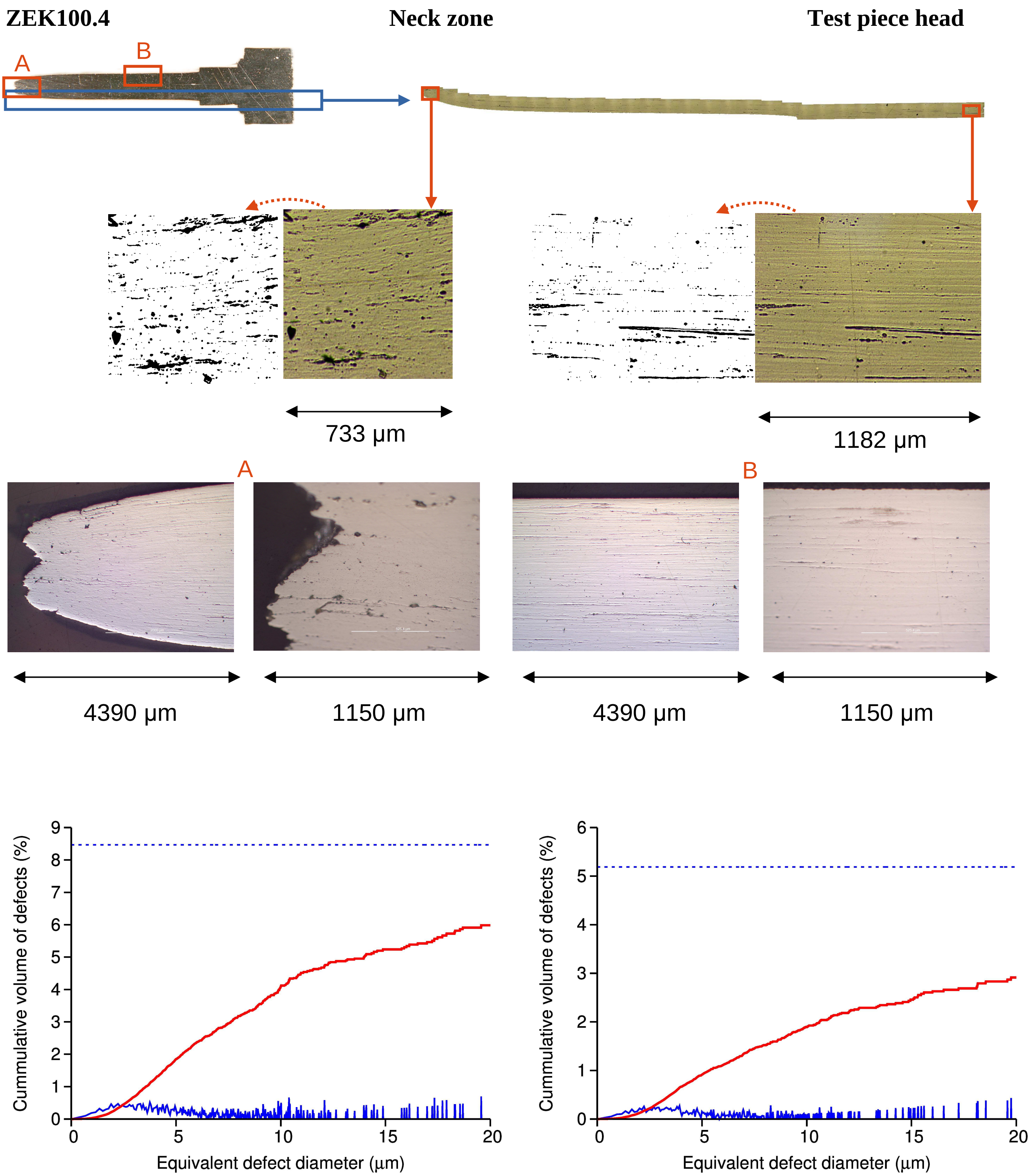
ZEK100.4
Neck zone
Test piece head
A
B
733 µm
1182 µm
A
B
4390 µm
1150 µm
4390 µm
1150 µm
Cummulative volume of defects (%)
Equivalent defect diameter (µm)
Cummulative volume of defects (%)
Equivalent defect diameter (µm)

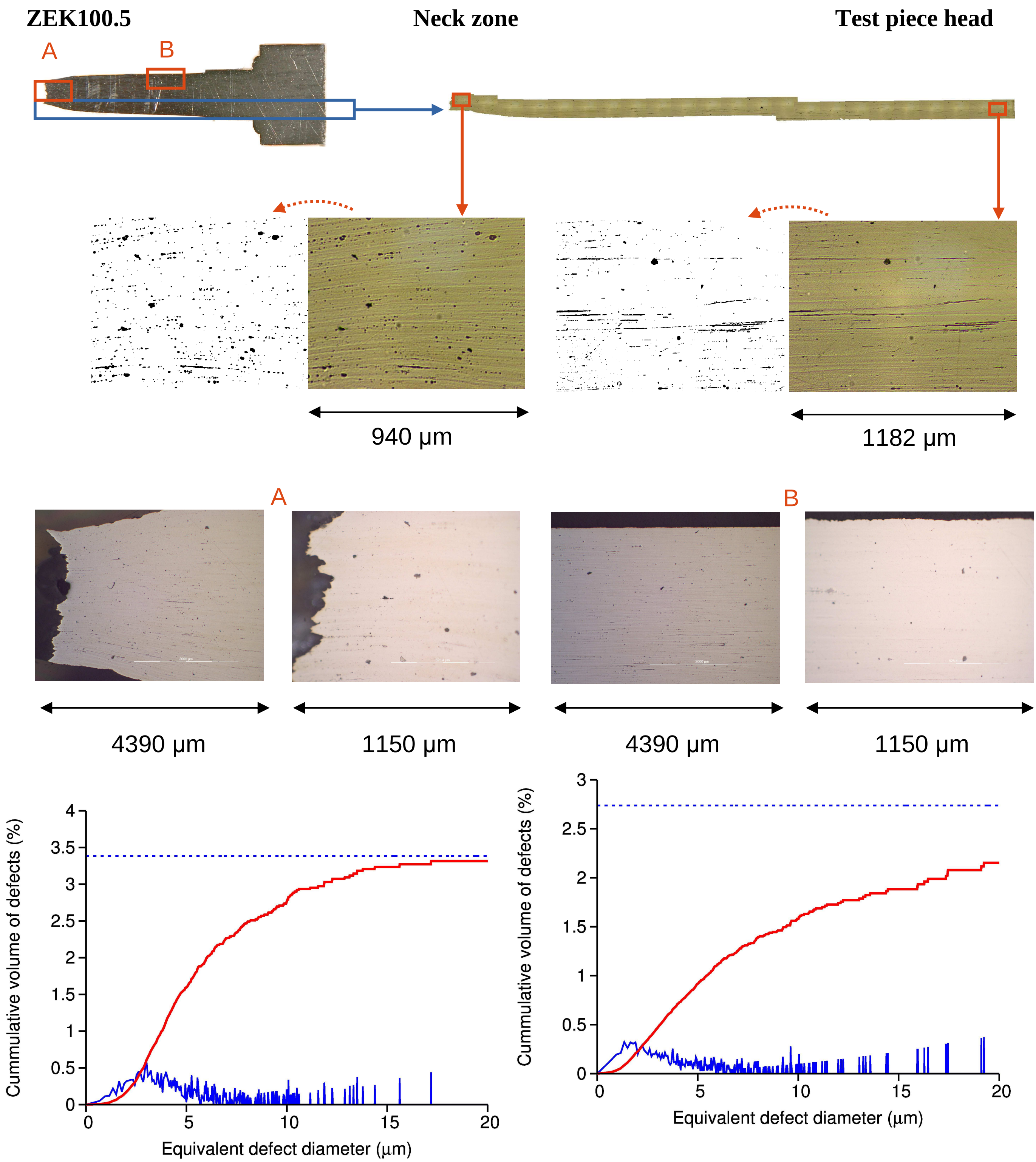
ZEK100.5
Neck zone
Test piece head
A
B
940 µm
1182 µm
4390 µm
1150 µm
4390 µm
1150 µm
Cummulative volume of defects (%)
Equivalent defect diameter (µm)
Cummulative volume of defects (%)
Equivalent defect diameter (µm)

2.4. Tubes

Al 36 tubes **Longitudinal section** **Cross section**

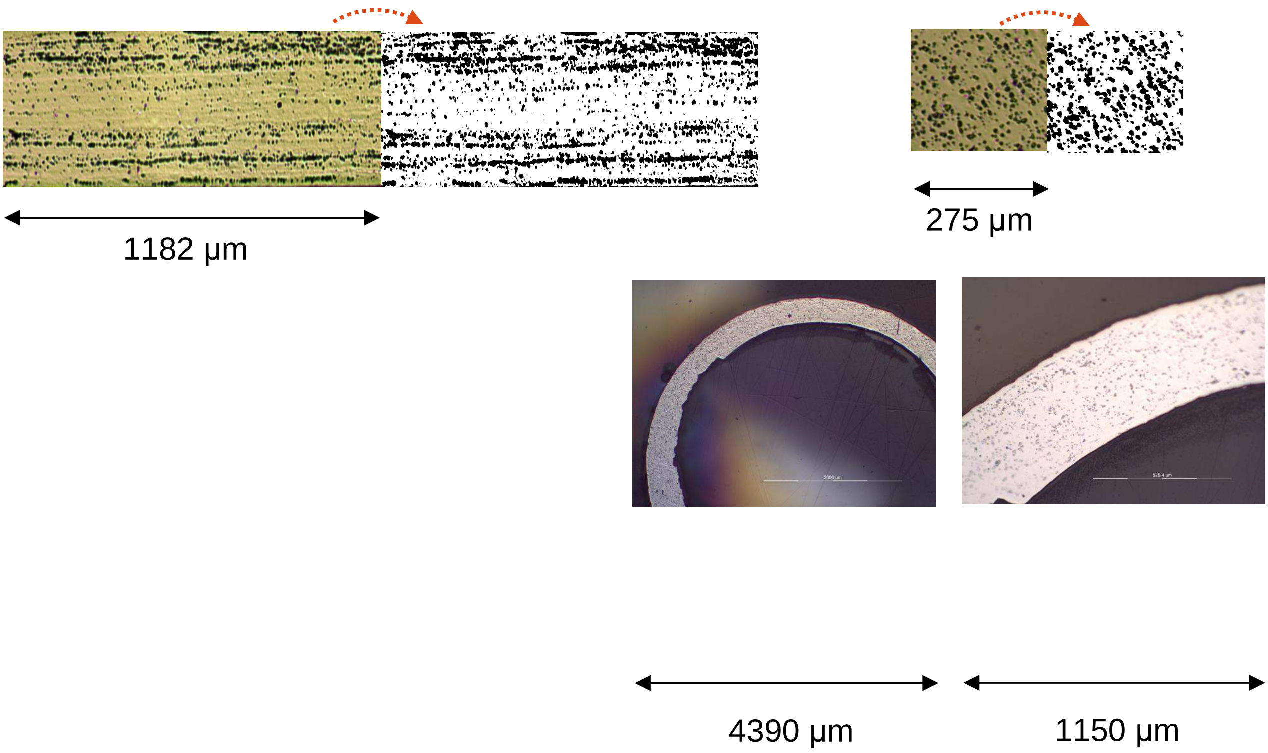

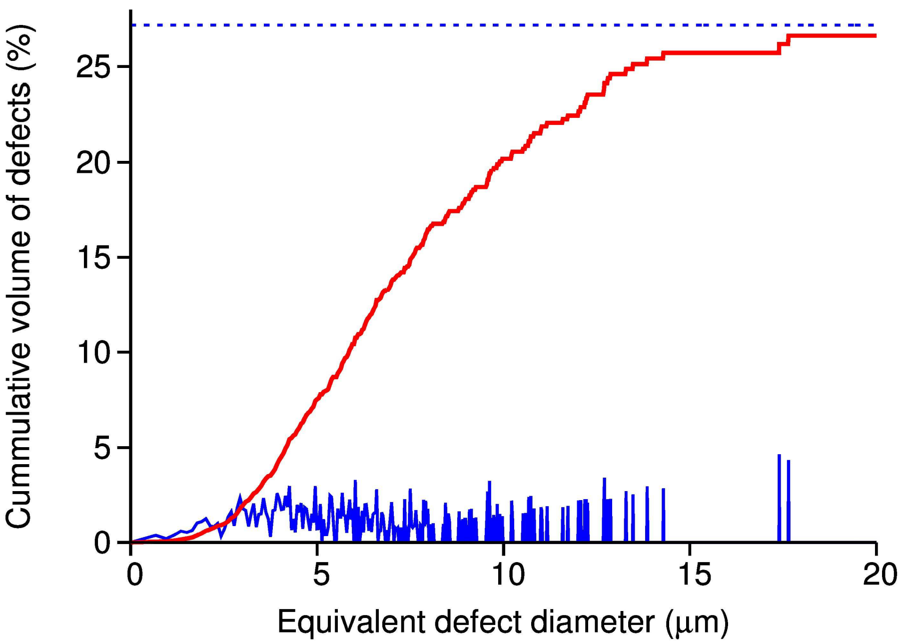

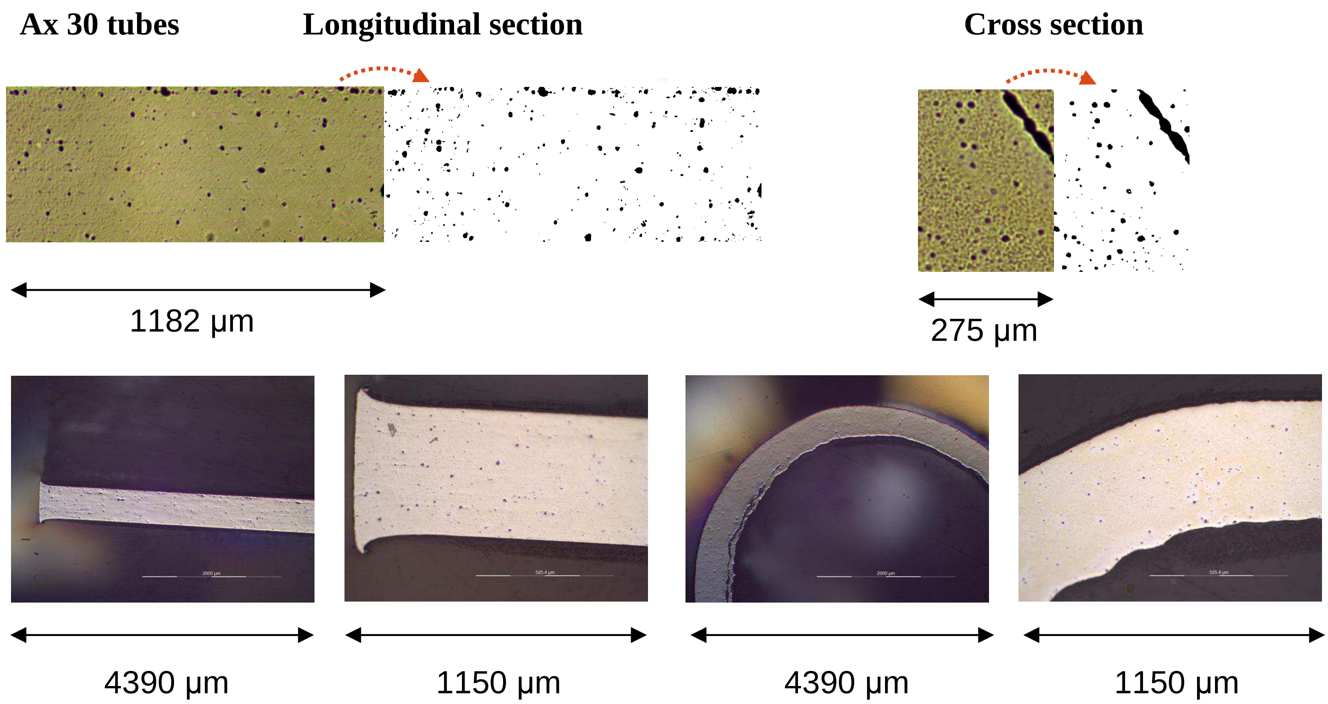
Ax 30 tubes
Longitudinal section
Cross section
1182 µm
275 µm
4390 µm
1150 µm
4390 µm
1150 µm

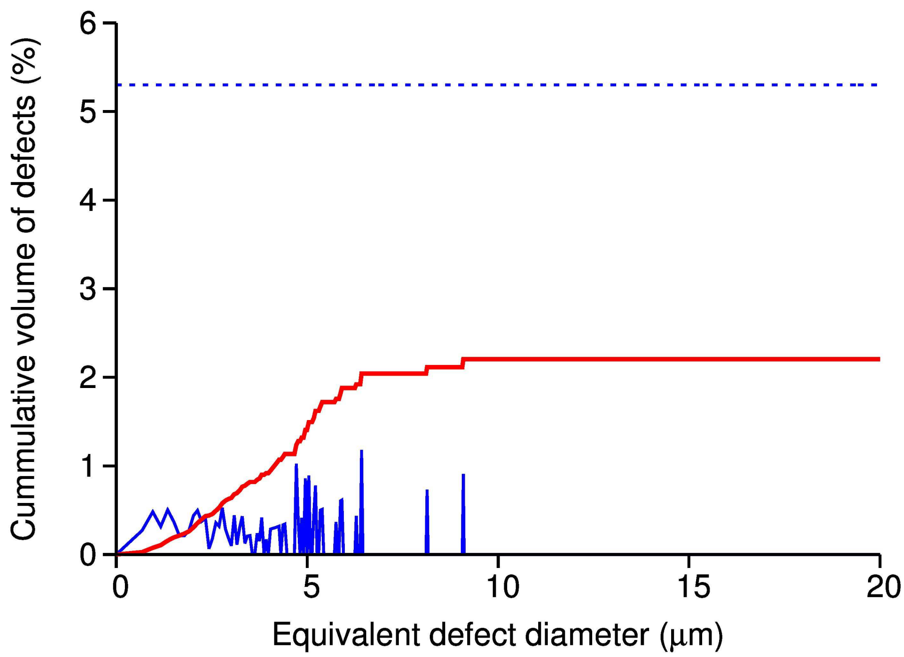
Cummulative volume of defects (%)
Equivalent defect diameter (µm)
0
1
2
3
4
5
6
0
5
10
15
20

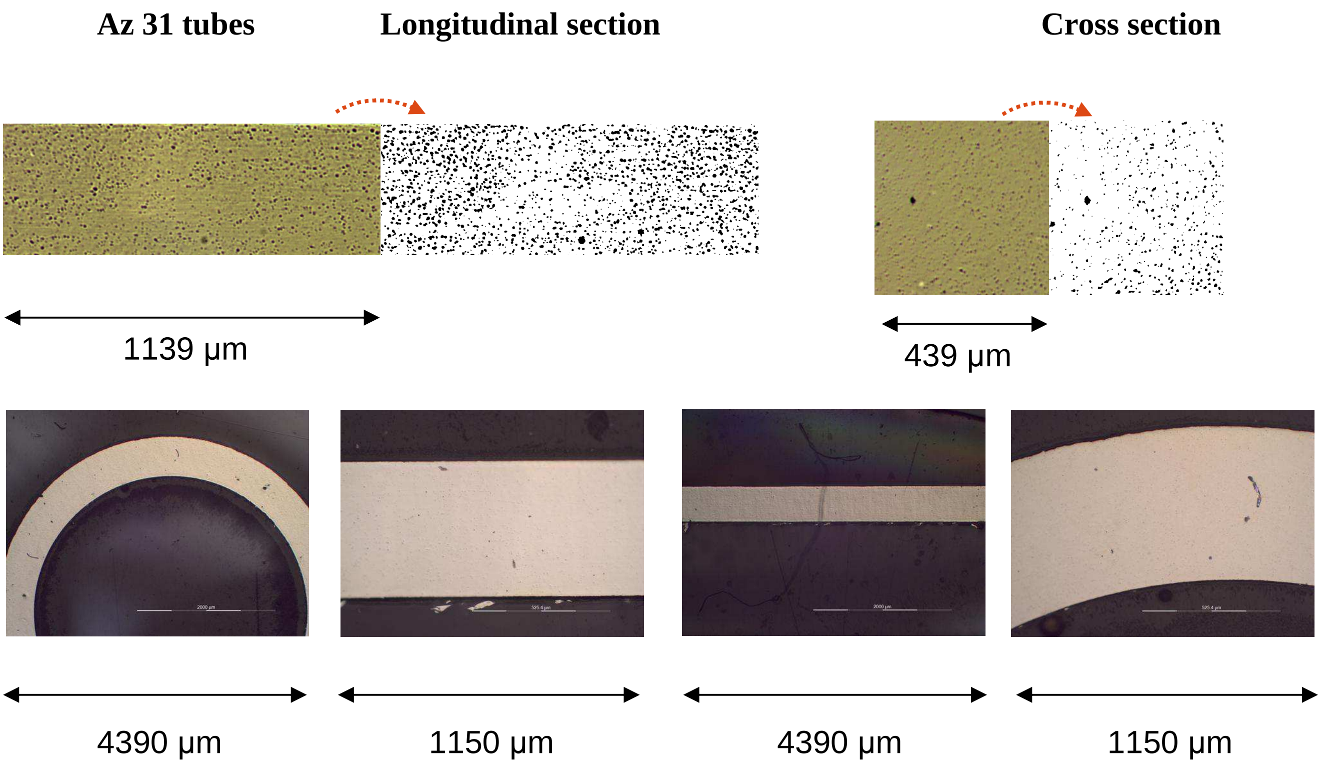
Az 31 tubes
Longitudinal section
Cross section
1139 µm
439 µm
4390 µm
1150 µm
4390 µm
1150 µm

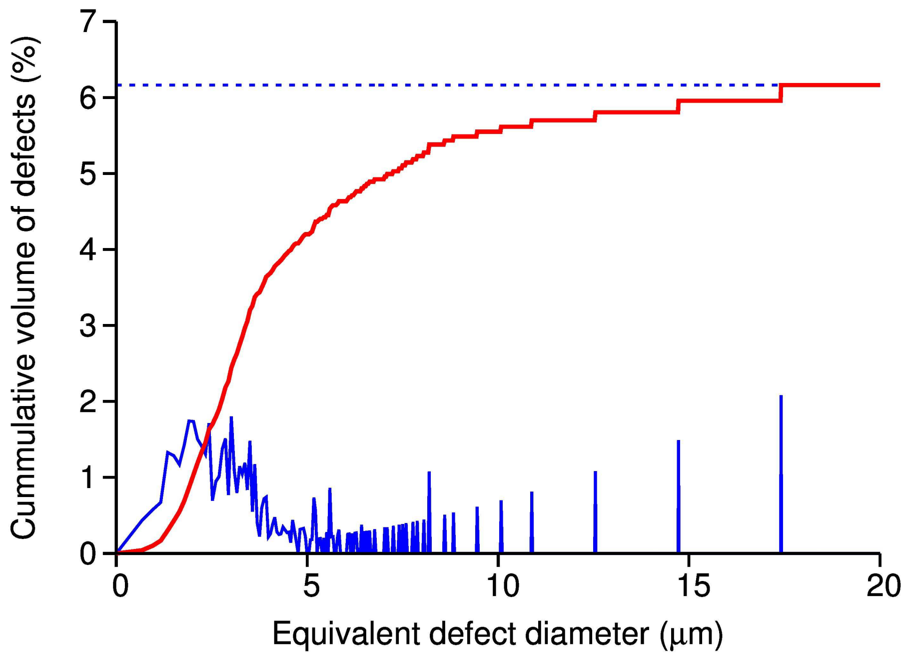
Cummulative volume of defects (%)
Equivalent defect diameter (µm)
0
1
2
3
4
5
6
7
0
5
10
15
20

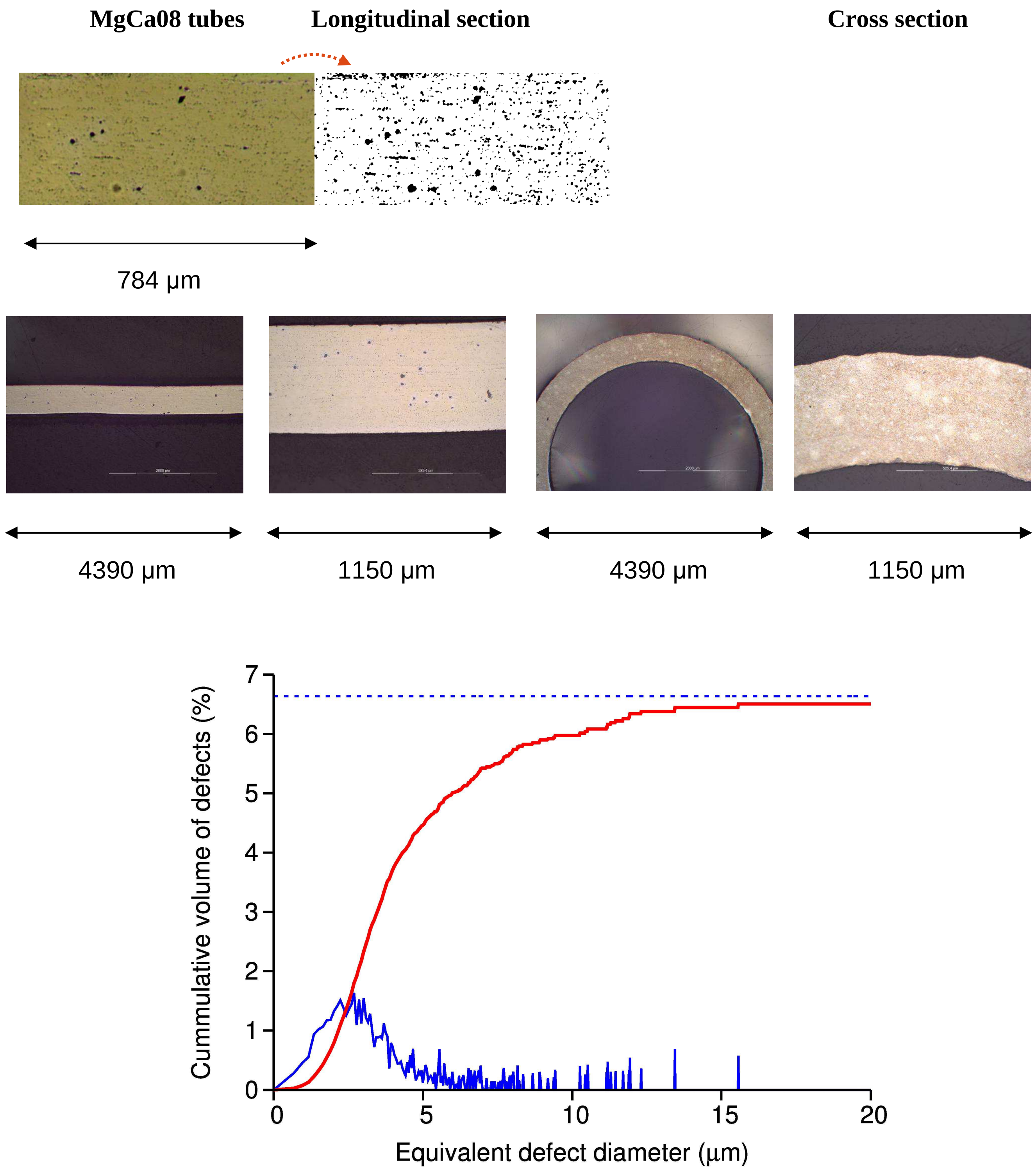

MgCa08 tubes
Longitudinal section
Cross section
784 µm
4390 µm
1150 µm
4390 µm
1150 µm
Cummulative volume of defects (%)
Equivalent defect diameter (µm)
0
1
2
3
4
5
6
7
0
5
10
15
20

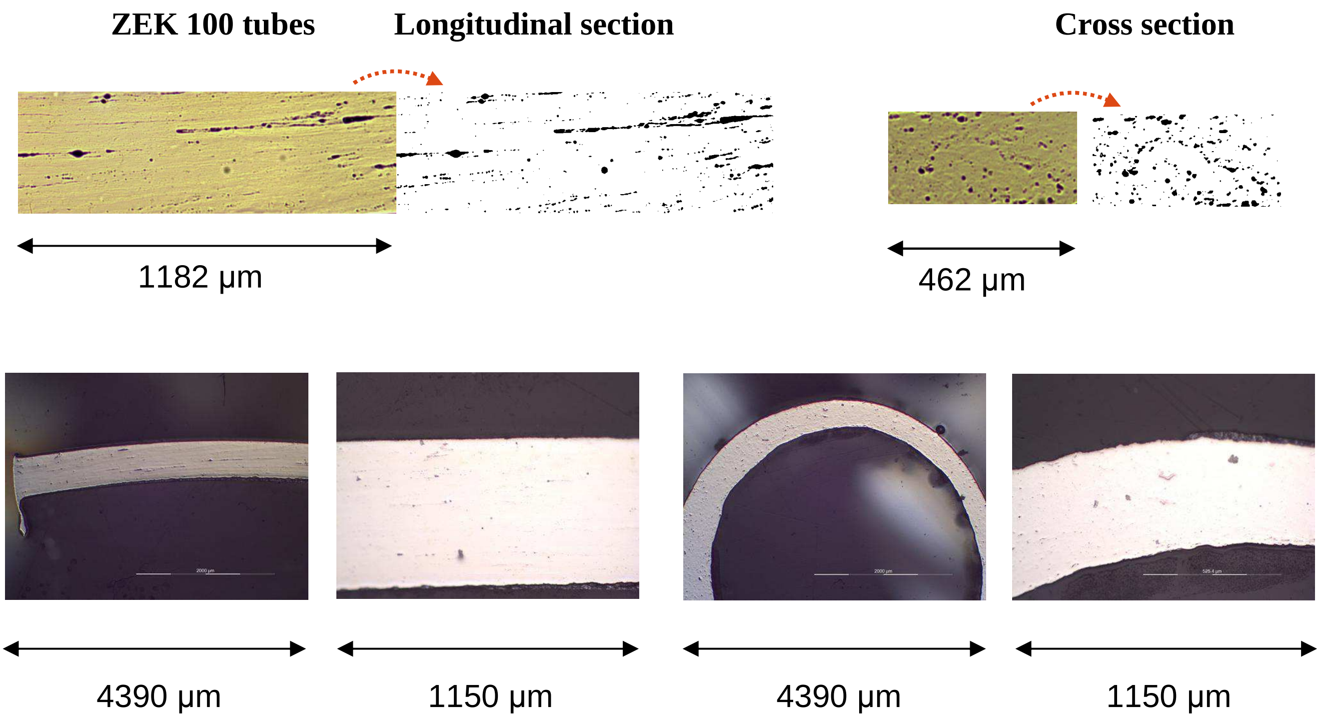
ZEK 100 tubes
Longitudinal section
Cross section
1182 µm
462 µm
4390 µm
1150 µm
4390 µm
1150 µm

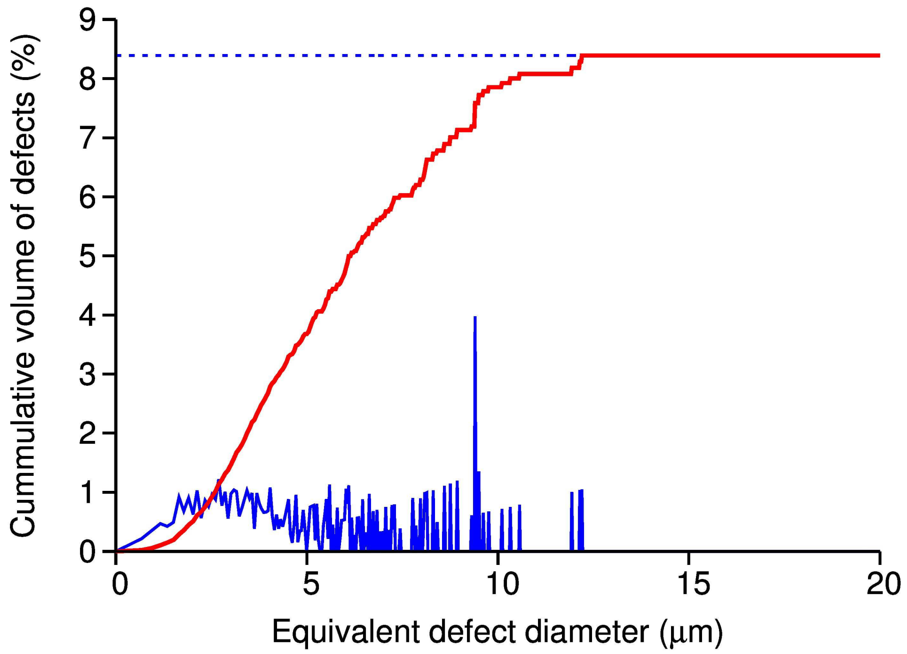
Cummulative volume of defects (%)
Equivalent defect diameter (µm)
0
1
2
3
4
5
6
7
8
9
0
5
10
15
20

2.5. Overall results from image analysis

Tab.1 Defects from image analysis on **tension bars, Ax30 alloys**. Resolution 1.2 μm/pixel.

	Neck zone			Test piece head		
	Defects	Image size [μm^2]	No. of images	Defects	Image size [μm^2]	No. of images
Ax30.2	1,9% (0,2)	886x1182	3	3,1% (1,0)	886x1182	4
Ax30.3	6,2% (1,4)	964x722	3	4,4% (0,6)	1182x886	3
Ax30.4	9,6% (3,7)	905x678	3	5,3% (1,6)	1182x886	3
Ax30.5	8,0% (1,7)	788x591	3	4,8% (0,3)	1182x886	3

Tab.2 Defects from image analysis **on tension bars, MgCa08 alloys**. Resolution 1.2 μm/pixel.

	Neck zone			Test piece head		
	Defects	Image size [μm^2]	No. of images	Defects	Image size [μm^2]	No. of images
MgCa08.2	3,1% (0,2)	918x688	3	3,2% (0,2)	1182x886	3
MgCa08.3	5,2% (0,8)	890x737	3	4,1% (0,5)	1182x886	3
MgCa08.4	4,3% (0,3)	944x875	3	2,6% (0,0)	620x467	2
MgCa08.5	3,8% (0,5)	790x875	3	2,7% (0,2)	1182x886	3

Tab.3 Defects from image analysis on **tension bars, ZEK100 alloys**. Resolution 1.2 μm/pixel.

	Neck zone			Test piece head		
	Defects	Image size [μm^2]	No. of images	Defects	Image size [μm^2]	No. of images
ZEK100.1	4,0% (0,4)	833x718	3	1,4% (0,5)	1182x886	3
ZEK100.2	4,6% (1,6)	817x516	3	1,6% (0,1)	1174x821	3
ZEK100.3	4,6% (1,4)	720x720	3	1,1% (0,3)	813x663	3
ZEK100.4	8,5% (0,7)	733x657	3	5,2% (0,8)	1182x886	3
ZEK100.5	3,4% (0,2)	940x749	3	2,7% (1,0)	1182x886	3

Tab.4 Defects from image analysis on **tubes**. Resolution 1.2 μm/pixel.

Tubes	Longitudinal section			Cross section		
	Defects	Image size [μm^2]	No. of images	Defects	Image size [μm^2]	No. of images
Al36	24,7% (1,5)	1182x304	2	27,2% (4,3)	275x248	3
Ax30	4,2% (1,3)	1177x381	2	5,3% (0,8)	258x347	2
Az31	12,9% (2,5)	1139x396	2	6,2% (2,5)	439x392	2
MgCa08	6,6% (1,4)	784x351	3	- -	-	-
ZEK100	4,3% (1,3)	1182x381	2	8,4% (0,2)	462x227	2

3. Three-point bending tests

Three point bending test on small pieces cut from tension bars heads were performed in a universal test machine. The sample dimensions were approx. 1.3 x 1.3 x 9 mm with a central notch (1/3 of the height) and L=7mm (Fig. 1, 2).

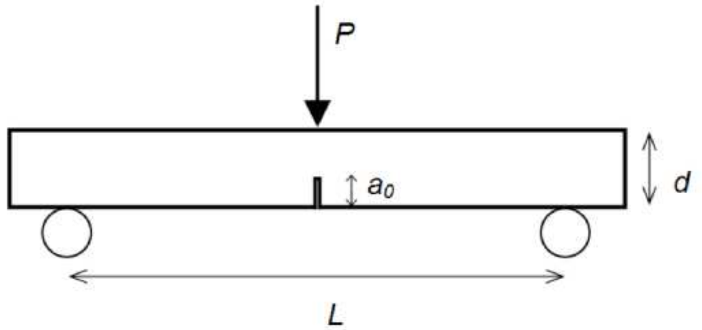

Fig. 1 Three-point bending geometry

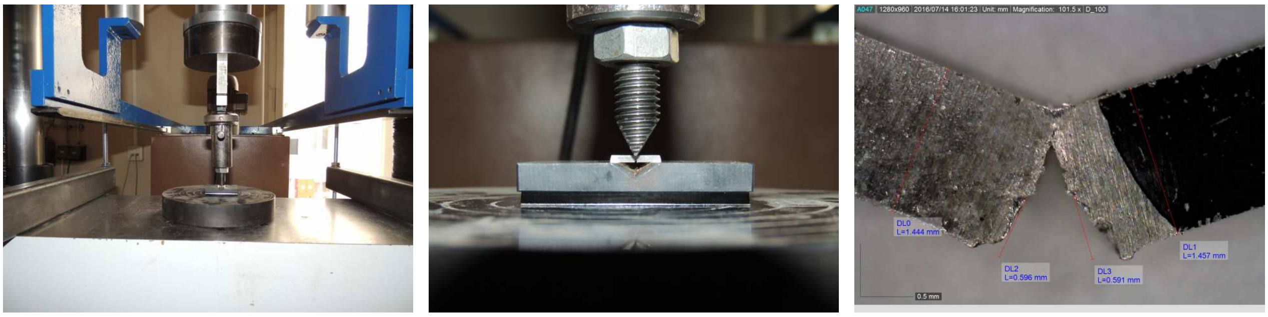

Fig. 2 Three-point bending instrumentation and fractured sample Ax30_31.

Work of external load was calculated such that the initial part of te load-deflection diagram was fittied witha linear function and the tail was approxiated with exponential function, (*f_lin(x)=a x+b* and *f_exp(x)=c* e^{dx}).

The work is given by

$$W_f = \int_0^{u_f} P \mathrm{d}u$$

From that, the average fracture energy in the ligament is defined as

$$G_f = \frac{W_f}{b(d - a_0)}$$

u.. deflection, *uf*...maximum deflection, *b*...sample width, *d*...sample height, *a0*...notch height.

Based on LEFM, fracture toughness can be calculated as
$K_{IC} = \sqrt{E \cdot G_f}$.

3.1. Results of three-point bending

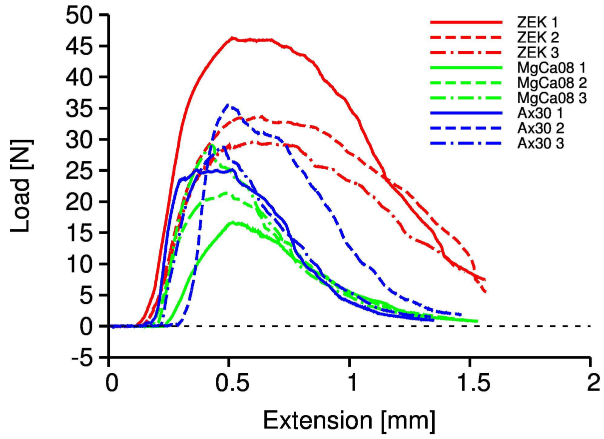

Fig. 3 Experimental load-deflection digrams.

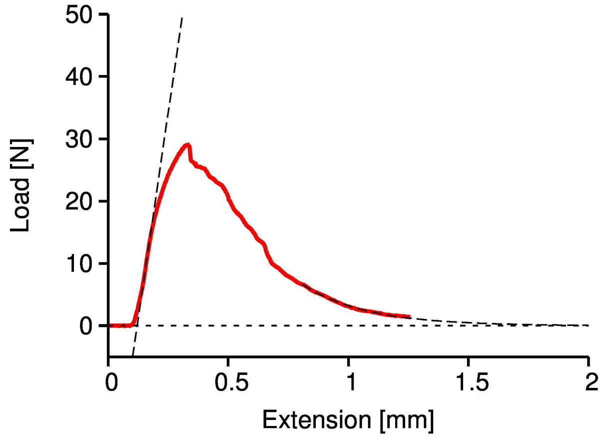

Fig. 4 Experimental load-deflection digram of MgCa08_3 with linear and exponential approxiamtions.

Tab. 5 Three-point bendnig results ("fracture energy")

Sample Label	**peak load**	**Gf**	**KIc**
	[N]	[N/m]	[MPa m^1/2]
Zek100.5_1	46.262	75974.54	58.471
Zek100.5_2	33.648	67116.872	54.957
Zek100.5_3	29.632	71251.243	56.624
MgCa08_1	16.67	17938.185	28.412
MgCa08_2	21.368	27420.604	35.127
MgCa08_3	29.02	26145.576	34.301
Ax30_1	25.138	14889.584	25.885
Ax30_2	35.522	25008.393	33.547
Ax30_3	28.776	17807.64	28.308

4. Nanoindentation

Tubes were tested by nanoindentation for the evolution of micromechanical properties across the specimens. Two types of cross sections were prepared:
i) c/s of a tube, i.e. indentation load imposed in the longitudinal (L) direction,
ii) longitudinal c/s, i.e. indentation load imposed in the hoop (H) direction, see Fig. 5

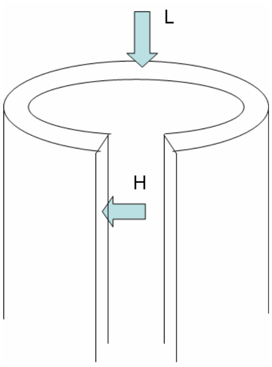

Fig. 5 Directions of indentation loading.

Testing parameters
Indentor: CSM-NHT, Berkovich or cube corner tip

Static indentation at load level Fmax= 5 mN, Loading/holding/unloading 5/10/5 s.

Four lines of equidistantly spaced indents prescribed for each sample coming from one end to another within the c/s.

Evaluated quantities

a. Hardness, H, defined as

$$H = \frac{P_{\max}}{A_c} \; .$$

where P_{max} is the maximum load, A_c is the projected contact area of the tip

b. Reduced/Young's modulus (Oliver and Pharr method)

$$E_r = \frac{1}{2\beta} \frac{\sqrt{\pi}}{\sqrt{A_c}} \left. \frac{dP}{dh} \right|_{h=h_{\max}}$$

Er is calculated directly form the unloading stiffness received from an experimental unloading curve. Er is further related to the Young's modulus by the following formula:

$$1/E_r = (1-\nu_i^2)/E_i + (1-\nu_s^2)/E_s .$$

where E_i, nu_i are Indenter's Young's modulus and Poisson's ratio, respectively and E_s, nu_s are sample Young's modulus and Poisson's ratio, respectively.

4.1. Nanoindentation results

Always, figures of indentation position is provided along with results of H and E from individual lines and average (thick line in graphs). The distance are given in micrometers.

Some fluctuations inside the cross section are dictated by the distribution of defects and also by intermetallics. In some cases, slight decrease of H or E (about 10% compared to mean) can be recognized in outer parts of the cross sectional area. In general, inner parts are stiffer compared to outer parts.

The effect of extrusion on the anisotropic micromechanical properties of the samples can be recognized. Always. the L direction is chracterized by 10-20% higher modulus and hardness compared to H direction.

4.1.1. Ax30 tube - L direction

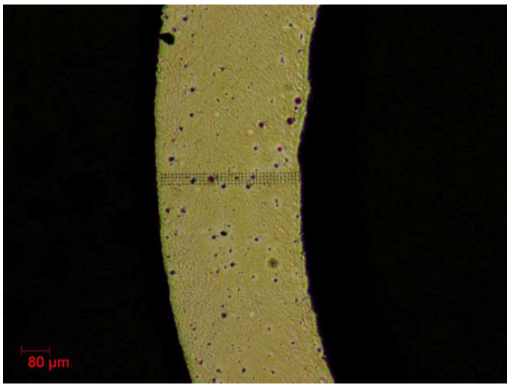

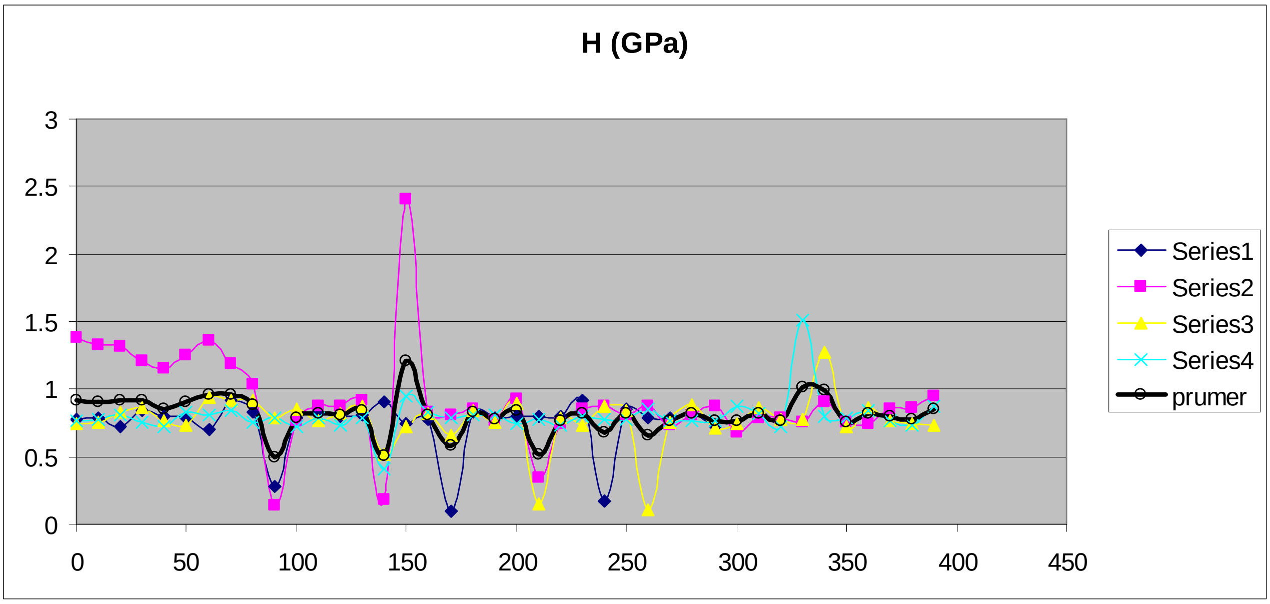

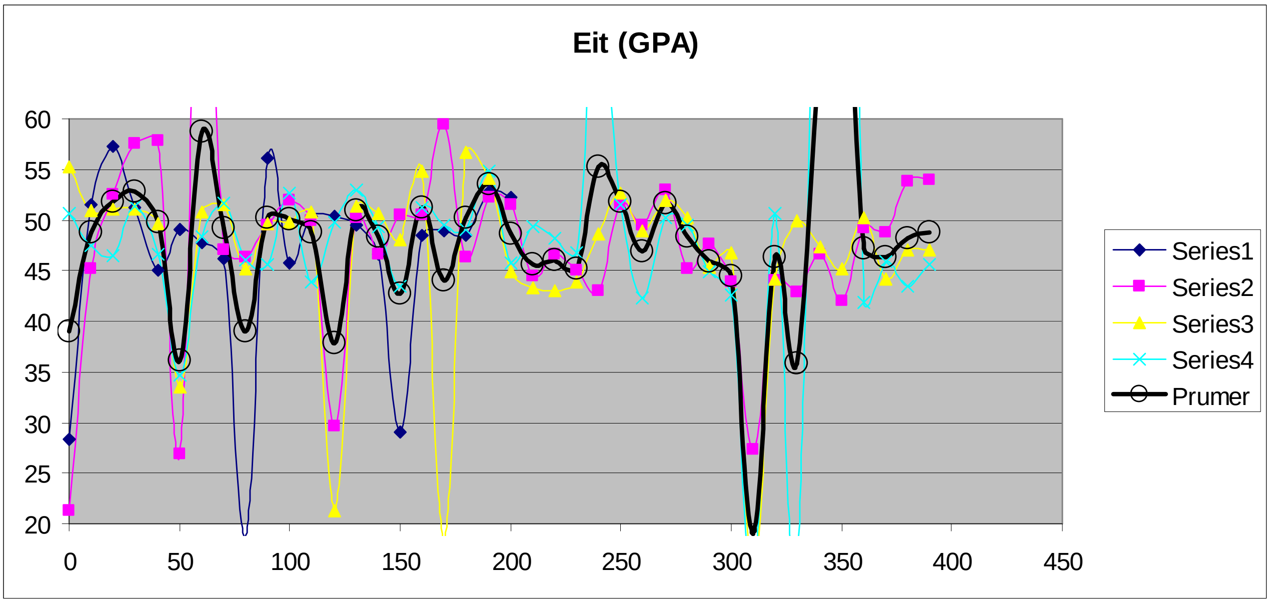
Eit (GPA)
60
55
50
45
40
35
30
25
20
0
50
100
150
200
250
300
350
400
450
Series1
Series2
Series3
Series4
Prumer

4.1.2. Ax30 tube - H direction

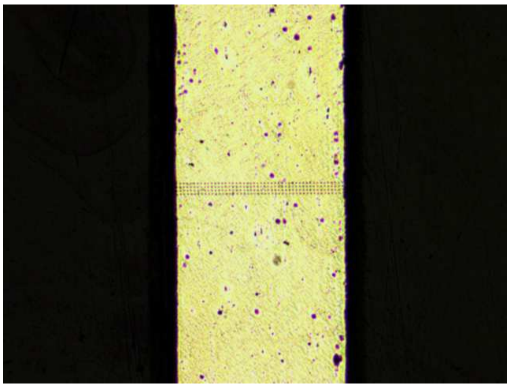

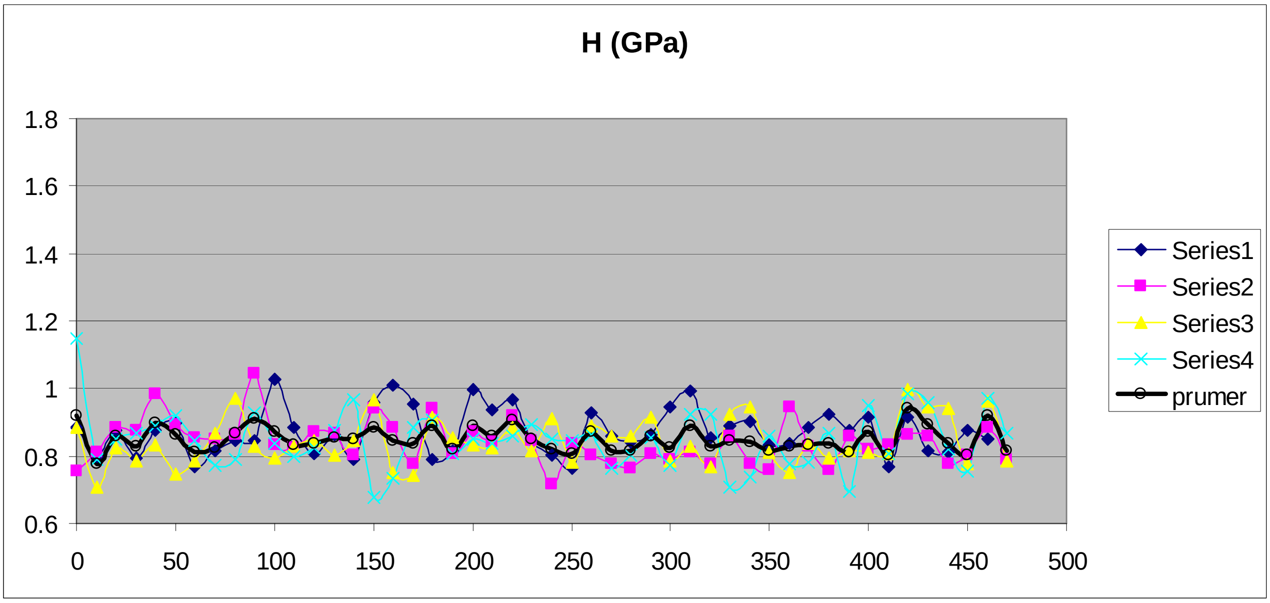

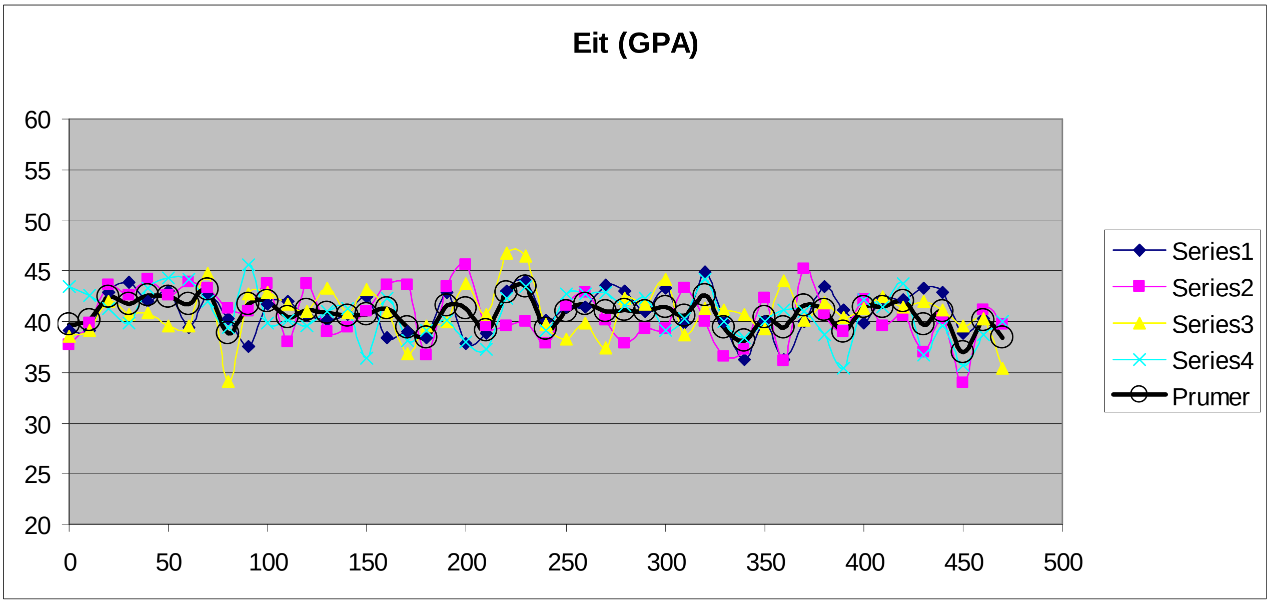

4.1.3 AZ31- L direction

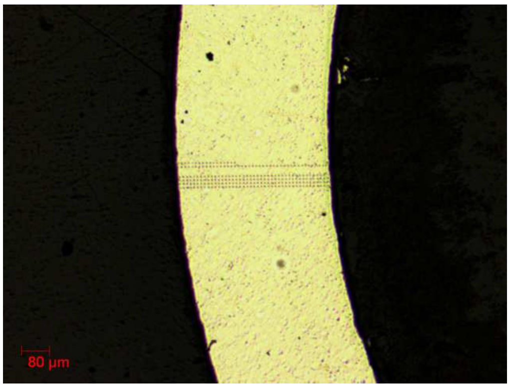

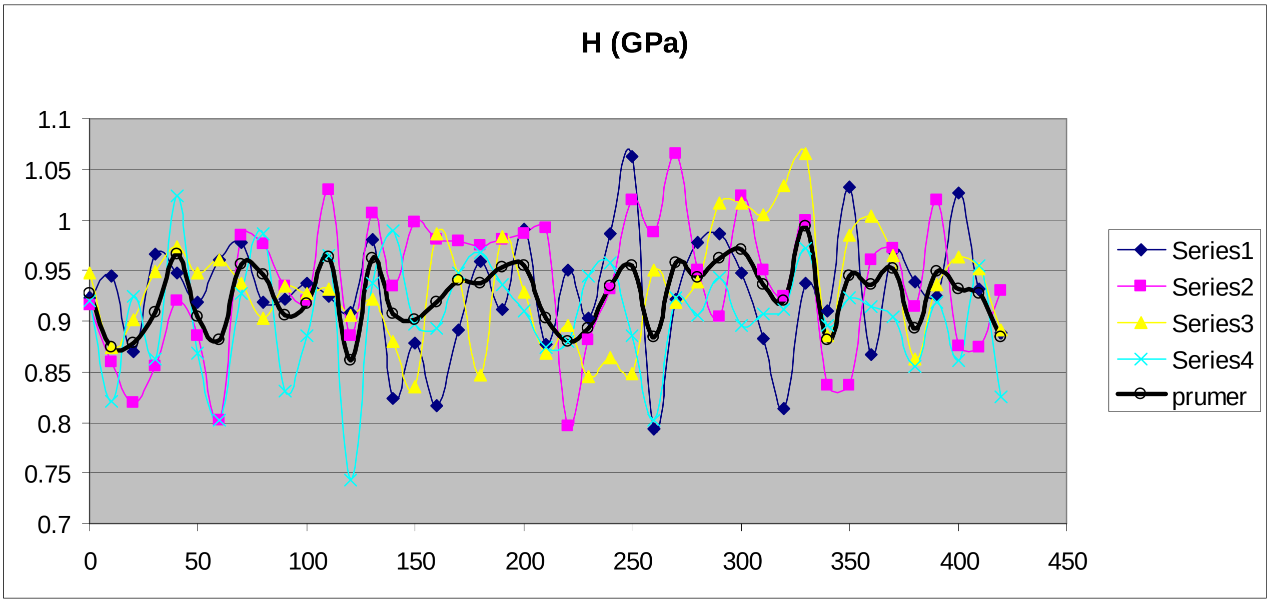

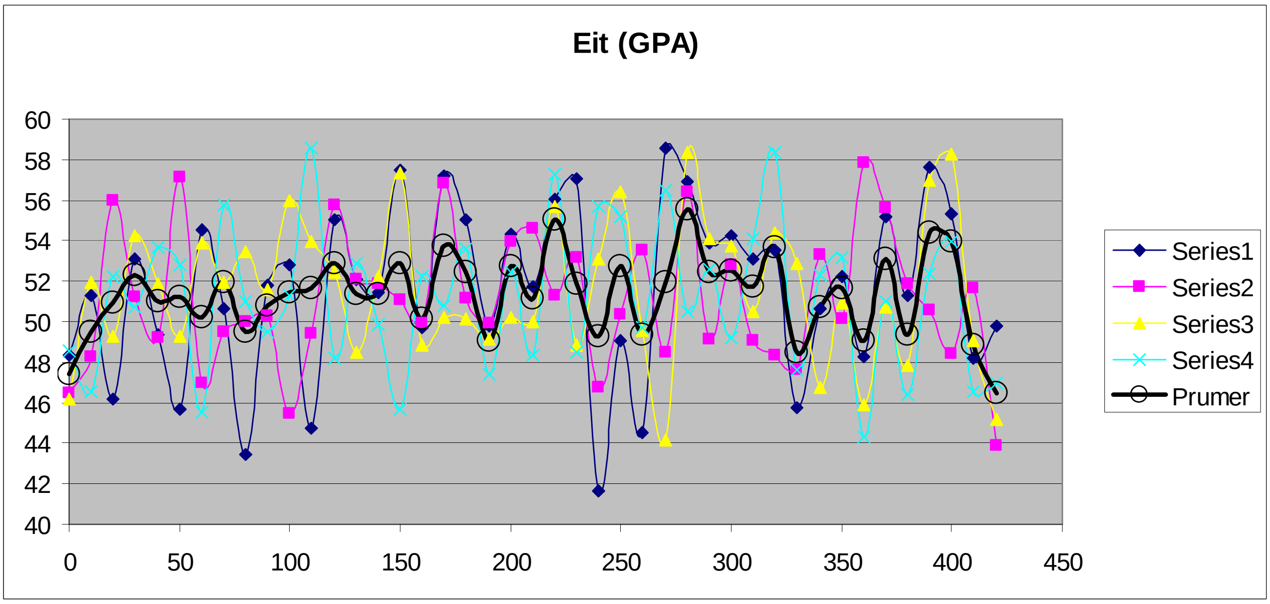

4.1.4. AZ31 - H direction

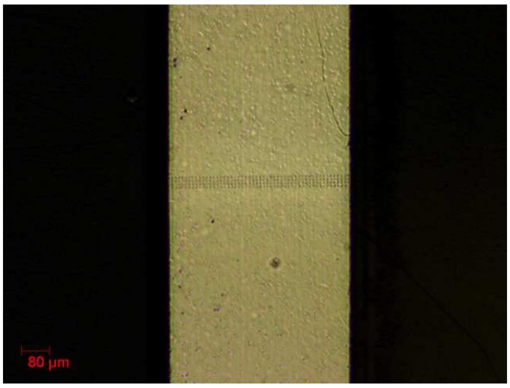

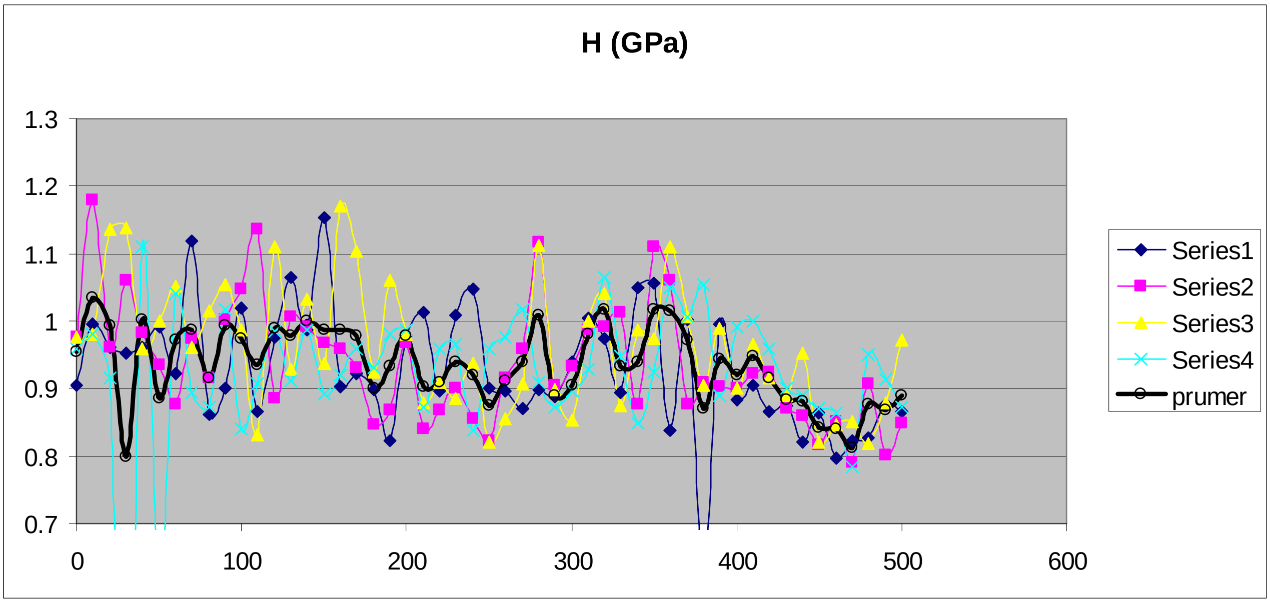

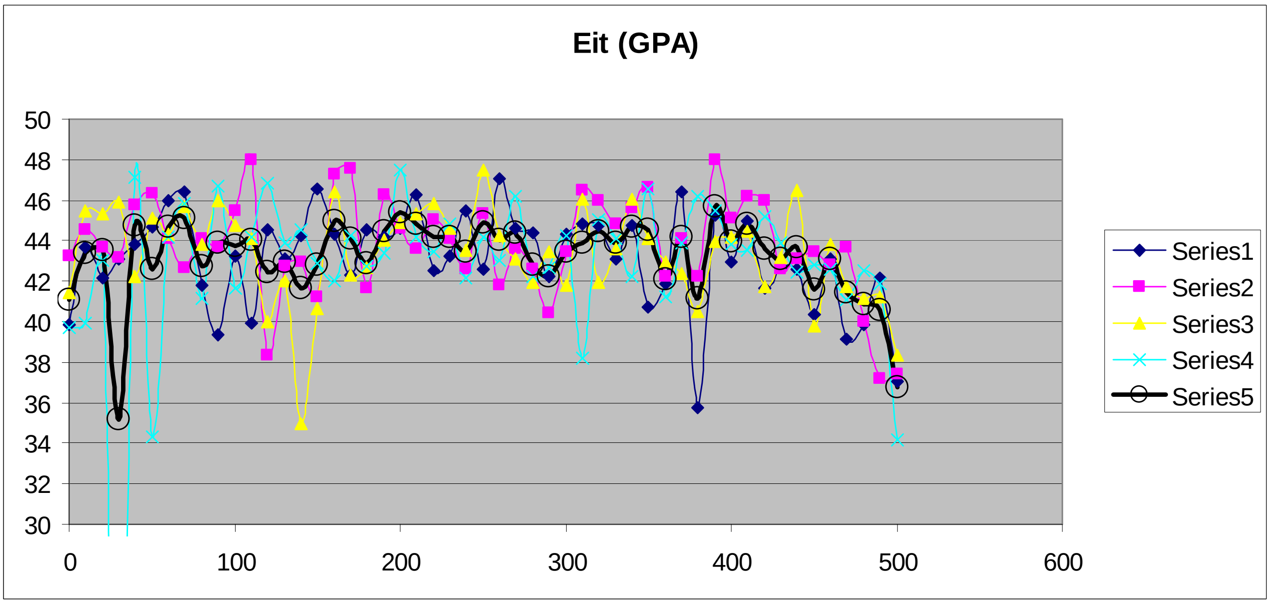

4.1.5. ZEK100 - L direction

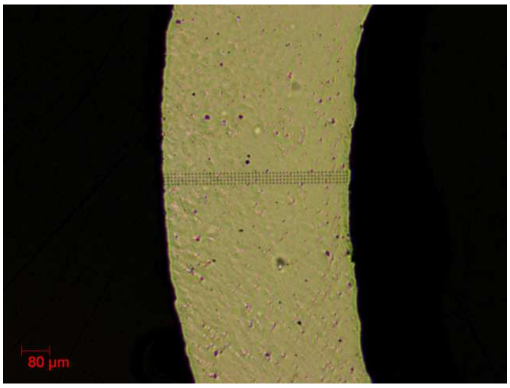

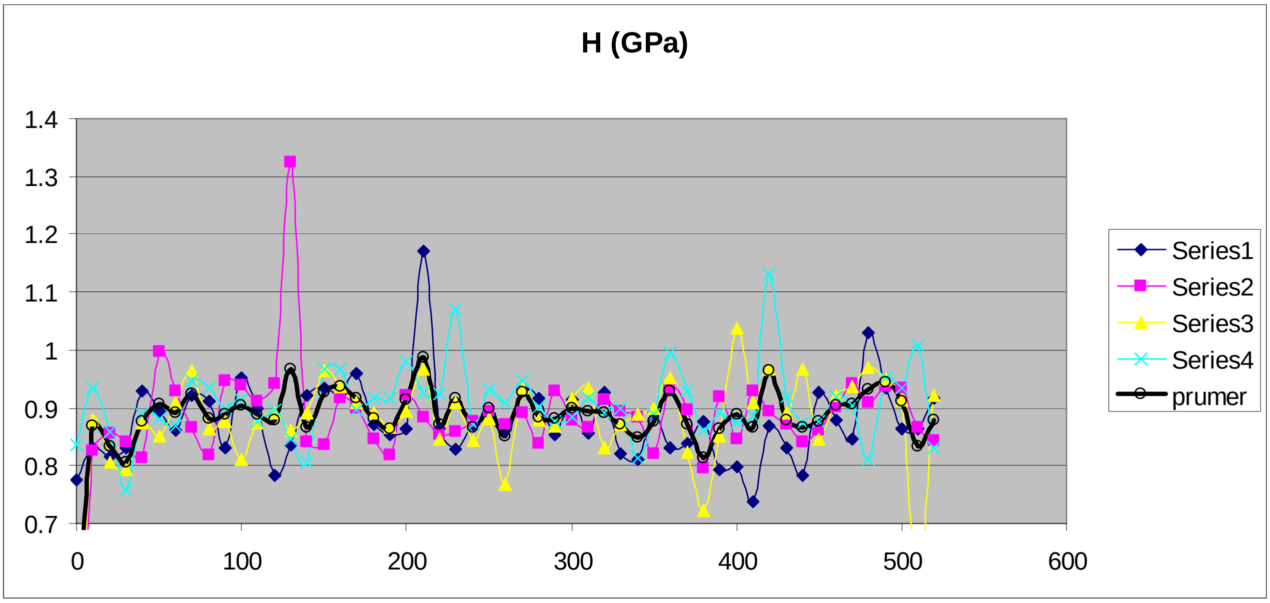

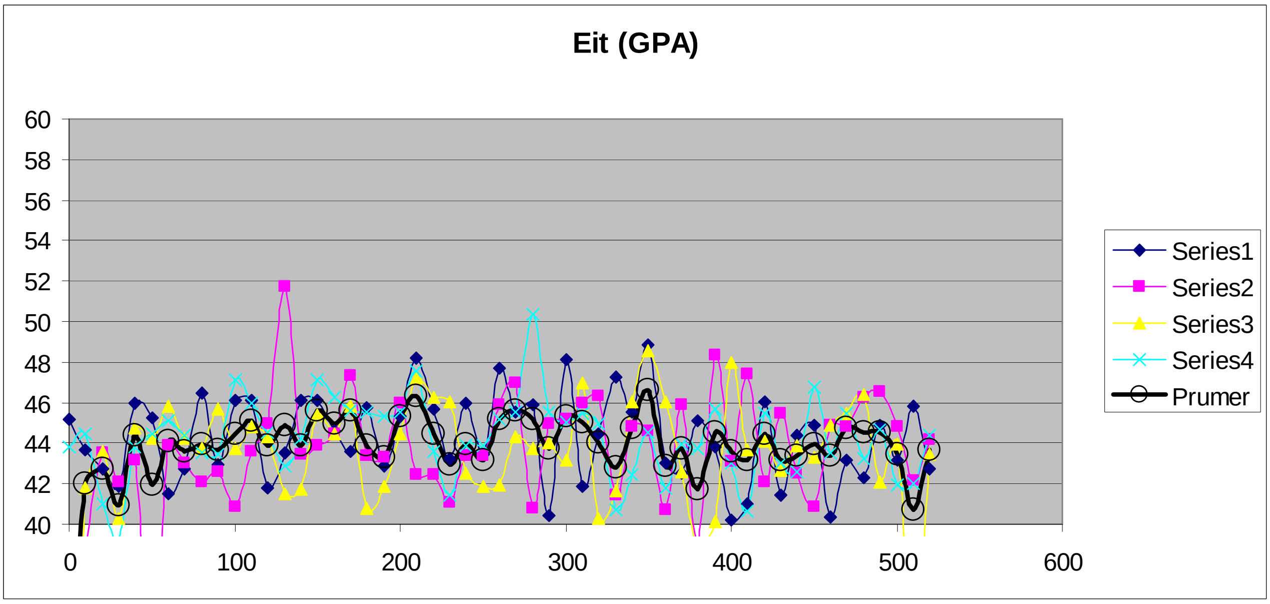

4.1.6. ZEK100 - H direction

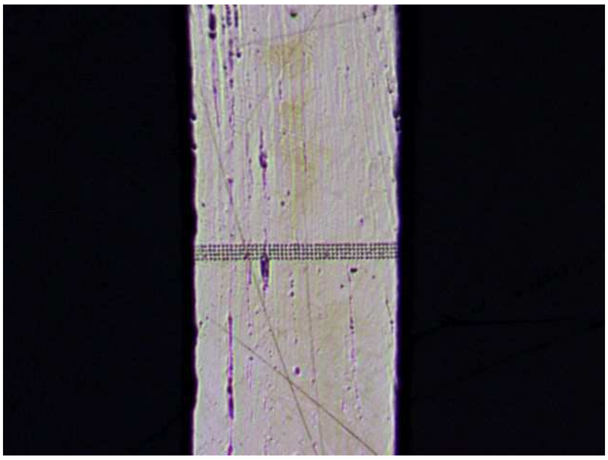

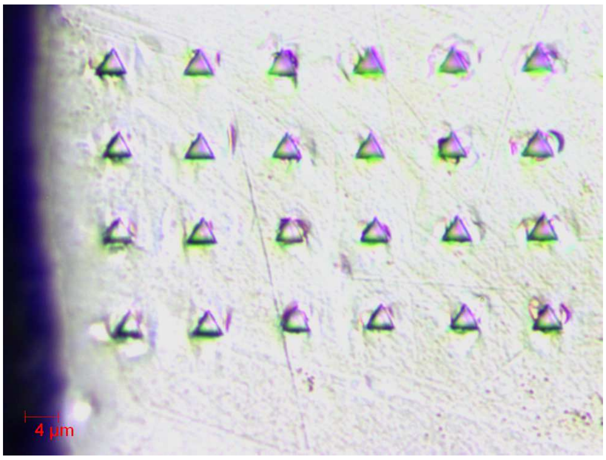

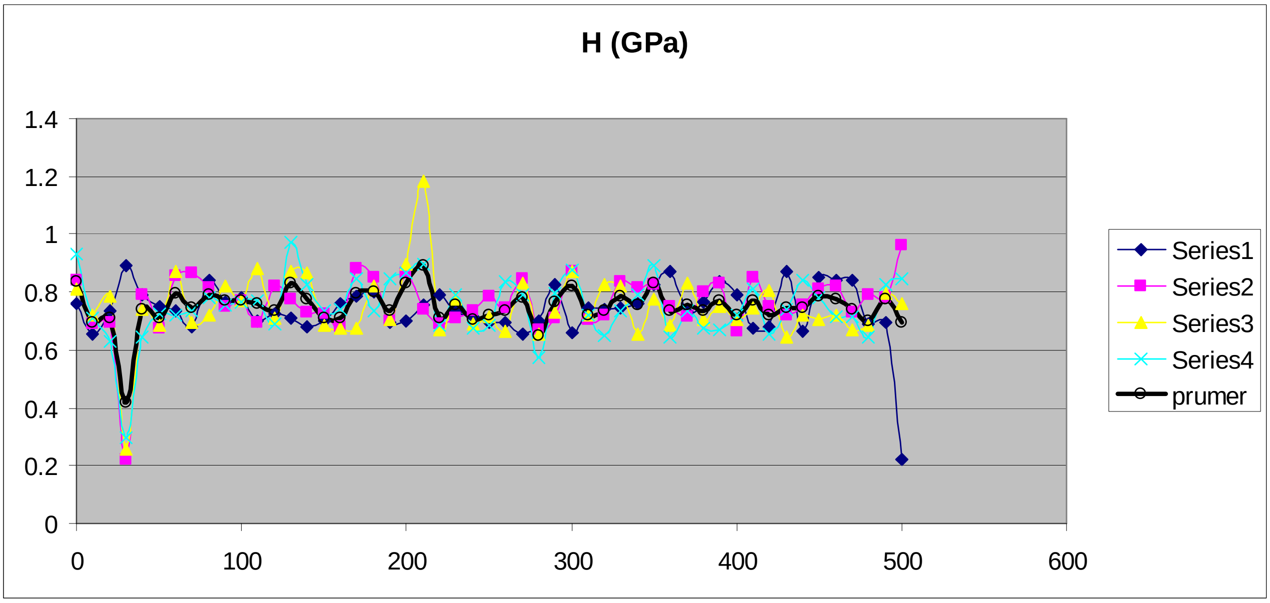

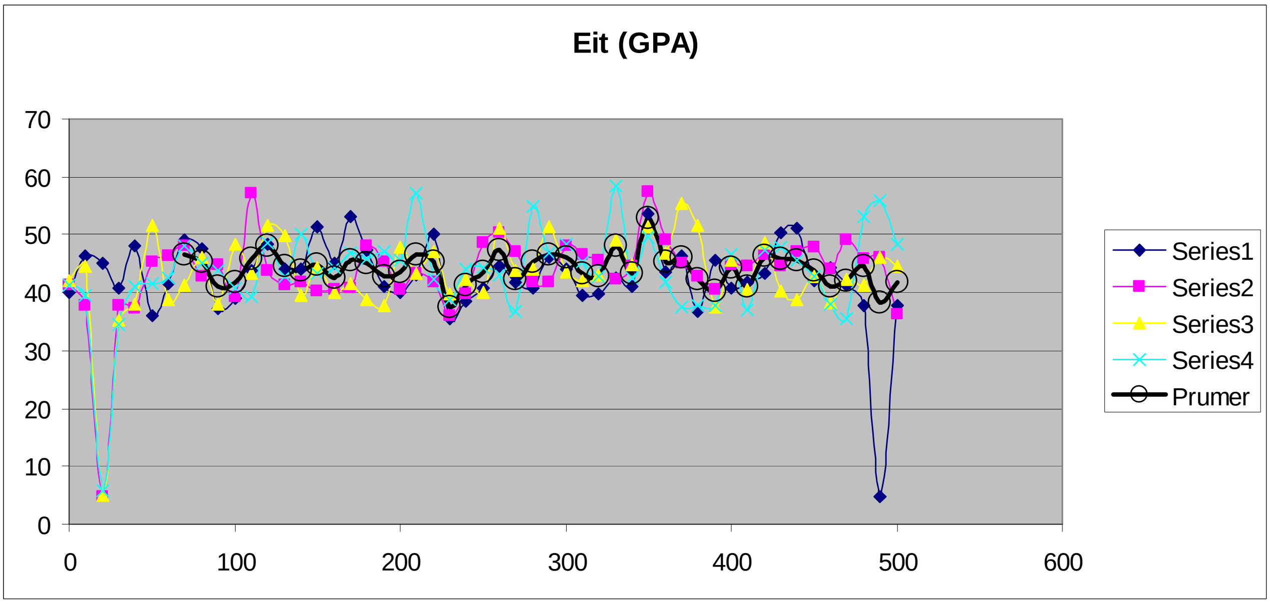

4.1.7. MgCa08 - L direction

no result yet.

4.1.8. MgCa08 - H direction

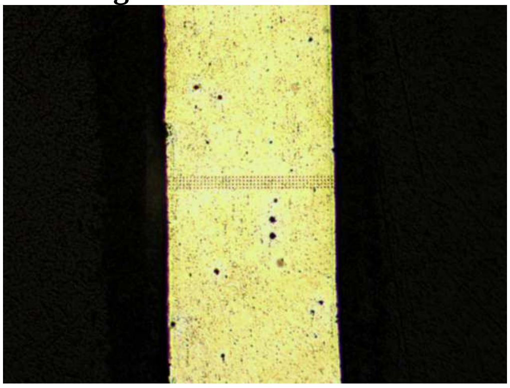

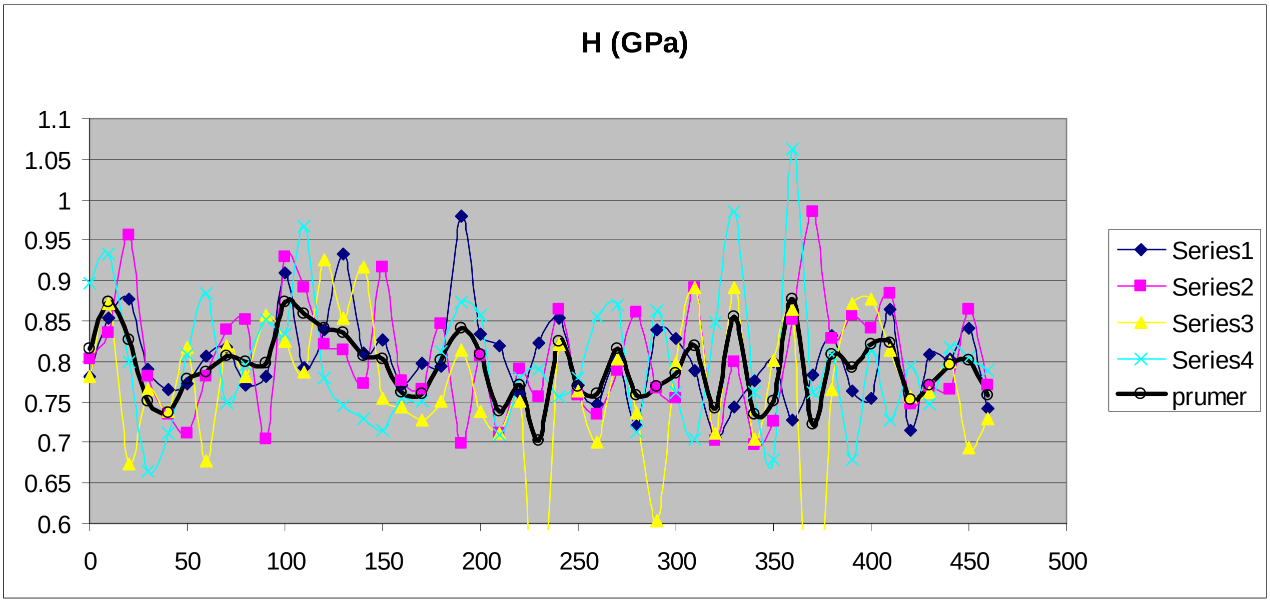

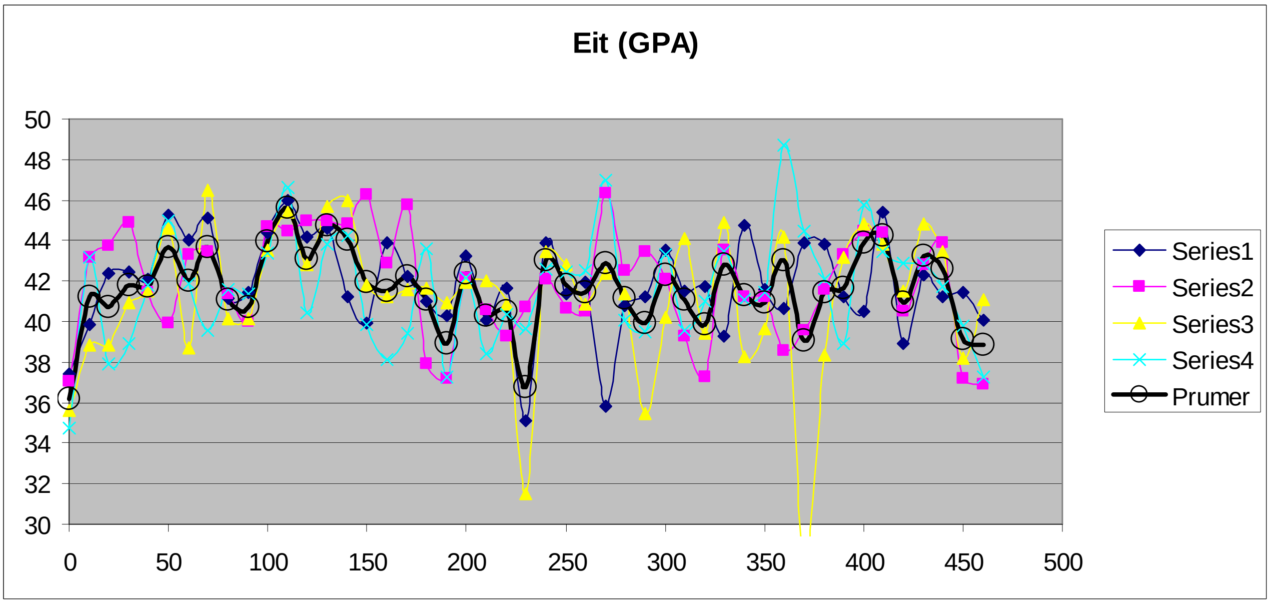

4.1.9. Ax36 - L direction

no result yet.

4.1.10. Ax36 - H direction